EXPERIMENTAL AND NUMERICAL INVESTIGATIONS OF AXIAL PULLOUT BEHAVIOR OF BURIED DUCTILE IRON PIPE

by

© Parththeeban Murugathasan

A Thesis submitted to the

School of Graduate Studies

in partial fulfillment of the requirements for the degree of

Master of Engineering

Faculty of Engineering and Applied Science

Memorial University of Newfoundland

October 2019

St. John's Newfoundland

ABSTRACT

Buried pipelines often cross active landslide areas, which are subjected to additional loads due to ground movements. The effect of ground loads on the performance of buried pipelines is an important consideration for pipeline integrity assessment. Though experimental and analytical studies were conducted to understand the maximum loads caused by the ground movement on the pipelines, design practices for the assessment of pipes subjected to ground movements are not yet well developed. This thesis presents the design of a new laboratory test facility developed for pullout testing of buried pipelines that investigate the behavior of pipelines subjected to axial ground movements. The test facility is first assessed using finite-element modelling to identify the effects of the size of the facility and the rigidity of the boundary walls on the pullout study of pipelines. The results show that a test cell having the dimensions of 2 m (width) x 1.5m (height) x 4 m (length) is adequate for the current purpose of tests if the wall stiffness is adequately designed. The facility is then used to conduct a pullout test of a 178-mm diameter ductile iron pipe. During the test, horizontal and vertical earth pressure in the soil is measured using Tekscan pressure sensors. Pipe deformation and wall strains are measured using strain gauges. A finite element modelling technique is developed to simulate the test conditions for investigating the soil-pipe interaction during the axial pullout test. The finite element model is then employed to study the pipe-soil interaction mechanism. The study reveals that arching effect and dilation of sand in the pipe–soil interface can affect the mobilized soil load on the ductile iron pipe. The unit interface shear resistance is found to be 16.0H to 17.0H in dense sand, 13.0H in medium dense sand and 5.0H in loose sand for the pipes tested.

ACKNOWLEDGEMENTS

Throughout my time spent in the master's program in the Faculty of Engineering and Applied Science at the MUN, I have come across numerous individuals who contributed to this amazing experience. First and foremost, I would like to take this opportunity to express my sincere gratitude to my supervisor Dr. Ashutosh Dhar for sharing his knowledge and experience, and for his continuous encouragement during the research program. His guidance has advanced my technical knowledge and critical thinking capability that helped me improve my overall confidence in this field. I would also like to thank my co-supervisor Dr. Bipul Hawlader, for providing me with geotechnical engineering expertise and invaluable suggestions. I thank him for his insights, time and attention.

I gratefully acknowledge the School of Graduate Studies, National Science and Engineering Research Council, FortisBC Energy Inc, SBM grants of the Memorial University of Newfoundland, Mitacs and PRNL for the financial support to undertake my master's study.

I would not have been able to have this opportunity to study at MUN without the recommendation given by Dr. George Mann. I will be forever grateful to him for his support toward this opportunity. I would also like to thank my friend, Dr. Maaran, and my wife, Dalshini, who helped and encouraged me during the course of this journey. I am also indebted to the lab technicians, and to fellow undergraduate and graduate students who supported me during the laboratory tests. Finally, I would like to thank my parents and friends for providing unconditional support and constant encouragement during this past two years.

Table of Contents

ABSTRACT ii

ACKNOWLEDGEMENTS iii

List of Figures viii

List of Tables x

List of Symbols xi

CHAPTER 1 1

Introduction and Overview 1

1.1 Background 1

1.2 Motivation 3

1.3 Objectives 4

1.4 Framework of Thesis 5

1.5 Key contributions 6

CHAPTER 2 7

Literature Review 7

2.1 Introduction 7

2.2. Studies on axial pipe-soil interaction 7

2.2.1 Experimental studies 7

2.2.2 Numerical Studies 12

2.3 Finite element modelling 12
2.3.1 Modelling techniques 13
2.3.1.1 Element types 13
2.3.1.2 Nonlinearities 14
2.3.2 Constitutive modelling of sand 15
2.3.2.1 Stress–strain behavior of sand 15
2.3.2.2 Mohr-Coulomb model 18
2.5 Summary 20
CHAPTER 3 21
A Laboratory Facility for Studying Pullout Behavior of Buried Pipelines 21
3.1 Abstract 21
3.2 Introduction 22
3.3 Review of Previous Studies on Laboratory Test Facility 23
3.4 Design of Test Cell 27
3.5 Numerical Modelling 29
3.5.1 Modelling Approach 29
3.5.2 Boundary Conditions and Loadings 31
3.5.3 Material Model and Parameters 32
3.6 Results and Discussion 34

3.6.1 Preliminary Analyses 34

3.6.2 Effect of Wall Distance and Wall Rigidity on the Soil Response 35

3.7 Summary 40

CHAPTER 4 46

An Experimental and Numerical Investigation of Pullout Behavior of Buried Ductile Iron Water Pipes 46

4.1 Abstract 46

4.2 Introduction 47

4.3 Test facility 49

4.4 Experimental program 52

4.4.1 Test materials and preparation 52

4.4.2 Test cell instrumentation 53

4.4.3 Test program 54

4.4.4 Test results 55

4.5 Numerical modelling of axial pullout 61

4.5.1 Finite element modelling 61

4.5.2 Soil parameters and material models 62

4.5.3 Comparison of results 65

4.6 Mechanism of soil-pipe interaction 67

4.7 Conclusions 72

CHAPTER 5 79

Summary and Recommendations for Future Work 79

5.1 Overview 79

5.2 Conclusions 79

5.3 Recommendations for Future Study 82

REFERENCES (General) 83

List of Figures

Figure 1.1. Anticipated modes of relative movement of pipe (Kariman 2006) 2

Figure 1.2. Schematic showing the buried pipes subjected to lateral and longitudinal ground loads (Kariman 2006) 2

Figure 2.1 Typical drained triaxial test results of dense and loose sand (a) Shear stress versus axial strain (b) Volumetric strain versus axial strain (Das 2008) 17

Figure 2.2. Mohr-Coulomb model in Abaqus (Abaqus 2016) 18

Figure 2.3. Mohr-Coulomb yield surface in the deviatoric plane (Abaqus 2016) 19

Figure 3.1. Schematic drawing of test cell's cross-section 28

Figure 3.2. Typical finite-element mesh of soil, test cell and pipe used in 2-D model 30

Figure 3.3. Typical finite-element mesh of soil, test cell and pipe used in 3-D model 30

Figure 3.4. Vertical stresses with soil depth, 0.2 m away from the cell wall (initial loading) 36

Figure 3.5. Vertical stresses with soil depth, 0.2 m away from the pipe centre during expansion 36

Figure 3.6. Deformation of test cell after gravity step 37

Figure 3.7. Deformation of test cell after simulation of dilation during the pullout 38

Figure 3.8. Horizontal soil stresses at springline level from pipe centre to cell wall 39

Figure 3.9. Vertical soil stresses at springline level from pipe center to the cell wall 39

Figure 4.1. Schematics of the test facility: a) test cell, b) a longitudinal section 50

Figure 4.2. Connection details between the pipe and hydraulic actuator 51

Figure. 4.3 Schematic view of test cell cross-section 52

Figure 4.4. Inner view of the test facility showing the pipe placement 53

Figure 4.5. Pullout force versus leading end displacement for Tests T1–T5.....56

Figure 4.6. Normalized pullout resistances (Tests T1–T4).....58

Figure. 4.7. Variation of soil stresses during axial pullout 59

Figure 4.8 Pipe wall strain during axial pullout.....60

Figure 4.9. Strain gauge readings on the side wall of the test cell during axial pullout 61

Figure. 4.10 Typical FE mesh used in finite element analysis 62

Figure 4.11 Comparison of full-scale test and finite element load–displacement responses in dense sand.....66

Figure 4.12 Comparison of full-scale test and finite element load–displacement responses in loose sand.....67

Figure 4.13 Axial strain along pipe length from FE analysis 69

Figure 4.14 Normal stress along pipe length from FE analysis.....69

Figure 4.15 Distribution of normal stresses around the pipe circumference 71

Figure 4.16 Plastic deformation of soil around the pipe.....71

List of Tables

Table 2.1 Friction factors for different pipe coatings (ALA 2001) 15

Table 3.1. Parameters used in FE analyses (design of test cell) 33

Table 4.1. Summary of pullout tests 55

Table 4.2 Parameters used in FE analyses (modelling of axial pullout).....64

List of Symbols

Symbols used in this thesis are listed in the relevant chapters as the thesis is written in manuscript format.

CHAPTER 1

Introduction and Overview

1.1 Background

Ductile iron pipes were introduced to the market to replace cast iron pipes in the early 1950s for transporting liquid and gas. The nominal diameter (internal diameter) of ductile iron pipes varies in the range of 3 inches (75 mm) to 64 inches (1600 mm) (AWWA C-151). These pipes made of ductile cast iron are generally manufactured with internal and external coatings to protect the pipes from corrosion. The ductile iron pipes are stronger than the original cast iron pipes. The life span of the pipes is expected to be more than 100 years (Kroon et al. 2004). The ductile iron pipes are commonly used in municipal water distribution system.

The buried pipelines are often exposed to various hazards during their service life. Ground loads generated on pipelines due to relative ground movement is one of the major hazards. Geohazards such as landslides and earthquakes cause relative ground movements and the associated ground loads. Depending on the orientation of the pipe against the direction of the ground movement, pipelines could be subjected to different modes of ground movements, as shown in Figure 1.1. The direction of ground movements can be either vertical, lateral, longitudinal, or any combination of these directions.

Due to these relative ground movements, external loads are caused on the pipelines. The schematics of the pipelines subjected to ground loads (longitudinal and lateral) along its length during landslides are shown in Figure 1.2. When the pipe is parallel to the direction

of ground movement, pipes are subjected to axial or longitudinal loads. If the pipe is oriented perpendicular to the direction of ground movement, lateral loads are exerted on the pipe.

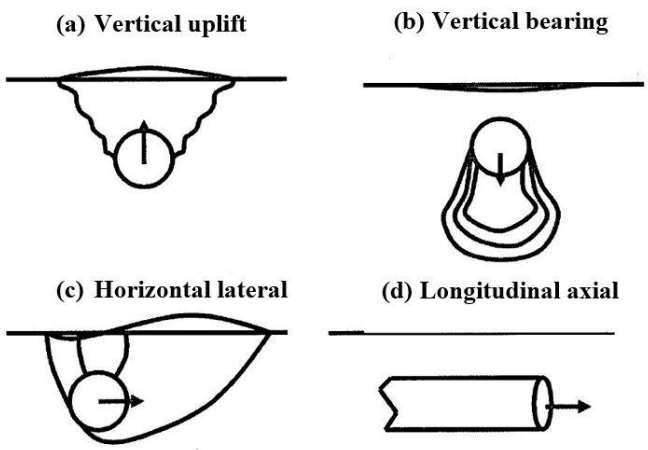

Figure 1.1. Anticipated modes of relative movement of pipe (Kariman 2006)

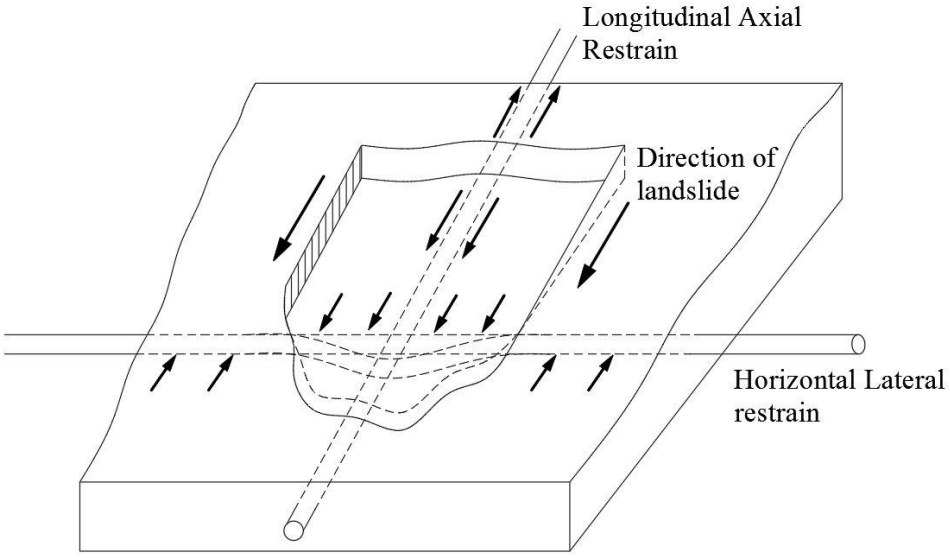

Figure 1.2. Schematic showing the buried pipes subjected to lateral and longitudinal ground loads (Kariman 2006)

Typically, in engineering practice, the pipeline routes are selected such that the likelihood of the geohazard is minimized. However, the placement of pipelines in areas that are prone to landslides is inevitable in some cases due to many reasons, such as environmental and political factors. Particularly, the municipal water distribution system is required in the communities, regardless of the exposure of the community to the geohazards. Therefore, certain design measures are considered during the design stage to make the pipelines resilient to the geohazards.

1.2 Motivation

Although the relative ground movement has been recognized as a geohazard for buried pipelines, the design method to account for the geohazard is not well-developed. A design equation (ASCE 1984) adopted almost 30 years ago has been the major design tool for the pipeline subjected to axial ground movement. This equation calculates the frictional resistance of soil at the pipe-soil interface for idealized conditions. Applicability of the design equation for steel energy pipelines was examined using various experimental studies (Sheil et al. 2018; Wijewickreme et al. 2009). This equation is found unsuccessful in predicting the maximum axial force on steel pipelines buried in dense sand (Sheil et al. 2018; Wijewickreme et al. 2009). Researchers also employed finite element modelling to understand the mechanisms of pipe-soil interaction for steel pipelines subjected to relative ground movements (Daiyan et al. 2011; Wijewickreme et al. 2009). However, ground loads on municipal ductile iron water mains are not extensively investigated. To this end, the current research is undertaken to develop a new full-scale test facility for investigation of

pullout behavior of buried pipelines and to experimentally and numerically investigate the response of municipal ductile iron pipes subjected to relative axial movements.

1.3 Objectives

This research aims to study the pipe-soil interaction behavior of buried ductile iron pipes during their axial movement. The main objectives of the study are to:

- Develop a laboratory test facility for pullout testing of buried pipelines to investigate pipes with different diameters, lengths, and materials, simulating the in-situ condition.
- Conduct full-scale laboratory tests to investigate experimentally the axial pullout responses of ductile iron pipes at various burial depths, relative compactions, and pulling rates using the developed facility.
- Develop a continuum-based finite element model to simulate the axial pipe-soil interaction behavior and validate the finite element model using the test results.
- Examine the pipe-soil interaction mechanism using the developed finite element model during axial pullout of ductile iron pipes.

1.4 Framework of Thesis

This thesis is organized in manuscript format. The outcome of the research is presented in five chapters. Chapter 1 presents the background of the problem, objectives, and significant contributions to the current research work.

Chapter 2 is a literature review that presents a general review of previous studies on the axial pullout of buried pipelines, stress-strain behavior of backfill sand and finite element modelling techniques. Since this thesis is written in manuscript format, a specific literature review relevant to each component of the study is presented in the corresponding chapters.

Chapter 3 presents the design of a new laboratory facility for pullout testing of buried pipelines. Finite element modelling of a test cell was carried out to assess the effect of boundary wall distance, boundary wall friction, and boundary wall rigidity during the axial pullout of buried pipelines, which are discussed in this chapter. This chapter has been published as a technical paper in the 71st Canadian geotechnical conference held at Edmonton, Alberta, Canada on September 23–26, 2018.

Chapter 4 presents the experimental and numerical investigation on axial pullout behavior of buried ductile iron pipelines. Five axial pullout tests of ductile iron pipes have been conducted using the developed test facility. Also, finite element modelling of axial pullout has been carried out, validating by the test results. This chapter has been submitted for publication in the Canadian Journal of Civil Engineering as a technical paper.

Chapter 5 presents the overall summary of the study with recommendations and suggestions for future works.

A separate reference section is provided to include the references cited in Chapters 1 and 2. References cited in Chapters 3 and 4 are included in the corresponding chapters as parts of stand-alone papers.

1.5 Key contributions

Conference paper

Murugathasan, P., Dhar, A. and Hawlader, B. 2018. A laboratory facility for studying pullout behaviour of buried pipelines. Annual conference of Canadian Geotechnical Society, GeoEdmonton2018, Edmonton, AB, Canada.

Journal paper

Murugathasan, P., Dhar, A. and Hawlader, B. 2019. An Experimental and Numerical Investigation of Pullout Behavior of Buried Ductile Iron Water Pipes. Canadian Journal of Civil Engineering (Under review).

Co-authorship Statement

All research work presented in the conference and journal papers were carried out by the author of this thesis, Parththeeban Murugathasan, under the supervision of Dr. Ashutosh Dhar. The first draft of the manuscript is also prepared by Parththeeban Murugathasan, and subsequently revised based on the co-authors' feedback and the peer-review process. As a co-author, Dr. Ashutosh Dhar and Dr. Bipul Hawlader provided support in developing the idea, provided guidance on finite element modelling, and reviewed the manuscript.

CHAPTER 2

Literature Review

2.1 Introduction

Ductile iron pipes, cast-iron pipes and polyethylene pipes are commonly used for water transmission and distribution systems in Canada and worldwide. Cast-iron pipelines were the major water transmission pipelines until the 1970s, which were or are being replaced by ductile-iron and polyethylene pipelines (Folkman 2018). There are thousands of kilometers of ductile iron pipeline networks that serve as the municipal water mains in Canada. These shallowly buried water mains are sometimes subjected to ground loads during any relative ground movement events. A detail investigation of these pipelines subjected to relative movement is an essential step to ensure the safe design of the pipe network and to improve the knowledge in pipe-soil interaction during the events. In this study, the relative axial movement of the ground is considered. This chapter presents a general overview of previous experimental and numerical studies reported on axial pipe-soil interaction behavior. Literature review specific to the works presented in Chapters 3 and 4 is given in each of the chapters.

2.2. Studies on axial pipe-soil interaction

2.2.1 Experimental studies

Experimental investigations on axial pipe-soil interactions of buried pipelines were reported by several researchers in the literature (e.g., Paulin et al. 1998; Wijewickreme et al. 2009; Daiyan et al. 2011; Sheil et al. 2018). Paulin et al. (1998) conducted full-scale

laboratory tests using steel pipes subjected to lateral and axial loadings buried in sand and clay. The sand used in their tests was well-graded with a coefficient of uniformity of 4, coefficient of curvature of 0.8, and maximum grain size of 4–5 mm. The tests were carried out in a loose state (D_r ~ 0%) and in a dense state (D_r ~ 100%) of the sand. The actuator used in their test had the 35-tonne pulling capacity and the pulling rate capability in the range of 0.5 to 10 mm/hr. They employed a pulling rate of 10 mm/hr. Experimental results showed that the effect of the relative density of sand backfill had a significant effect on the mobilized soil resistance. In loose-fill conditions, normalized peak relative pipeline load was 0.3 whereas in dense conditions it was close to 1.

Wijewickreme et al. (2009) conducted some full-scale laboratory tests on a sand-blasted steel pipe (457 mm diameter) buried in the Fraser River sand. The Fraser River sand used in their tests had the average grain size of 0.23 mm and coefficient of uniformity of 1.5. The peak friction angle in the range of 43.5° to 45.5° was measured using the laboratory triaxial tests. The critical state friction angle in the range of 31° to 33° were assumed based on the previous studies (Uthayakumar 1996). Based on a specially conducted direct shear tests (a steel coupon was mounted to the bottom part of the direct shear box at the top surface, and the upper shear box was filled with the sand), the interface friction angle of 33° and 36° were measured for loose and dense sand, respectively. The relative density, D_r, of the sand was maintained at 25% and 75% for loose and dense sand, respectively. Pipe burial depth of the tests conducted in dense sand was 2.5 times the pipe diameter and in loose sand was 2.7 times the diameter. The pipe was pulled in a displacement-controlled manner at the pulling rate in the range of 2 to 50 mm/s. Normal stresses on the pipe were

measured using total pressure transducers. Normalized soil resistance, $F_A^{'}$ (average shear stress around the pipe/vertical effective overburden pressure at the pipe centerline pipe), in the range of 1 to 1.1 was obtained for the tests conducted in dense sand conditions while 0.42 was obtained for loose sand. The maximum pullout forces from the tests were higher than those calculated using ALA (2001) equation for pipes in dense sand. The measured interface normal stresses were higher than the average normal stress calculated using the vertical and lateral stress (ALA 2001).

Bilgin and Stewart (2009) have conducted full-scale field tests using cast iron pipe buried in sand to investigate the axial pipe-soil interaction. The cast iron pipe used in their study has an outside diameter of 175 mm and a length of 3.66 m. A trench was excavated in the field, and a test compartment was built using 15.9-mm plywood sheets. The excavated trench had dimensions of 1.22 m (depth) x 1.22 m (width) x 6.71 m (length). The axial pullout tests were conducted with two types of backfill densities. The sand was compacted with the relative compaction of 95% (based on the standard proctor maximum dry density) to obtain the dense state. The average dry unit weight of dense backfill was 18.4 kN/m^3 with the average moisture content of 5.8%. The average dry unit weight of loose backfill was 14.8 kN/m^{3,} with the average moisture content of 5.3%. The pipe burial depth was 0.76 m. The outcomes of their tests showed that dense fill develops a peak soil resistance of 10.1 kPa and loose-fill develops a peak resistance of 4.6 kPa. A simple model was proposed to estimate the interface shearing resistance in terms of a constant and cover depth. The interface shearing resistance was found to be 6.0*H*, 9.3*H* and 14.0*H* (*H* is the

cover depth measured from the center of pipe) for loose, medium, and dense sand, respectively. The constant values depend on backfill properties.

Daiyan et al. (2011) studied the axial–lateral interaction behavior of a steel pipe buried in dense sand using centrifuge tests. The inner dimensions of the centrifuge model were 1180 mm × 940 mm × 400 mm. A pipe having a diameter of 41 mm with a length to diameter ratio of 8 was used in the test. The cover depth of the pipe was 61.5 mm. The equivalent prototype length of the pipe and the cover depth was 504 mm and 1008 mm, respectively. The tests were conducted under a centrifugal acceleration of 9.3g and the displacement rate of 0.04 m/s. Minimum and maximum void ratios of dry fine silica sand used in the tests were 0.6 and 0.93, respectively. The average density of sand was 1598kg/m^3. The peak friction angle of 43° and the critical state friction angle of 33° were estimated using laboratory direct shear test results. Further, the pipe-soil interface friction coefficient was found to be 0.44. The test conducted with pure axial load showed that axial interaction factor increases with the pipe displacement up to a distance of 0.34 times pipe diameter. It was reported that an axial interaction factor of 1.4 is necessary while assuming the at-rest earth pressure coefficient is 1.0 to match the peak axial resistance.

Sheil et al. (2018) tested the buried steel pipe subjected to cyclic axial loads using a full-scale laboratory facility. The test cell was developed with the internal dimensions of 1.83 m (depth) × 0.95 m (width) × 1.31 m (length) using 25-mm marine plywood panels. Two stiffened steel face panels with compressible foam seal around the pipe were used at the front and back end of the test cell to let the pipe settle during the cycling loading. In

addition, a 10-mm thick steel plate was used at the top of the test cell to apply additional loads using pressure bags. The steel pipe used in their study had an external diameter of 350 mm and a thickness of 6 mm. The pipe was split into three sections to minimize the end effects during the pullout. The middle section had a length of 500 mm and attached to a separate load cell using a 'spindle' support structure which runs through the inside of the pipe. An epoxy coating was applied to the center portion of the pipe surface. Two different types of sand (Houston HN31 and sand K) were used in the tests. The Houston sand had a median particle size of 0.35 mm, a coefficient of uniformity of 1.7, a peak friction angle of 37.9°, and a critical state friction angle of 35.4°. The sand K had a median particle size of 0.19 mm, a coefficient of uniformity greater than 2.5, a peak friction angle of 36.8°, and a critical state friction angle of 30.5°. The depth of soil cover in the tests was varied in the range of 0.35 m to 1.2 m. The findings of their study showed that the axial resistance increased with the increasing overburden pressure during the first cycle. The normalizing approach was proven to be inappropriate to compare the test results with different cover depth or overburden pressure. The tests conducted using Houston sand showed an increase in soil resistance when a narrower trench was used. Also, the test results proved the significance of pipe weight and trench wall friction on the mobilized soil loads. Normal stress measurements on the pipe surface showed that initial normal stress on the pipe crown was 20% higher than the nominal overburden pressure due to the rigid inclusion effect. The prediction of axial soil resistance using ALA (2001) method were in agreement with the test results for some tests when the at-rest lateral earth pressure coefficient (K_0) was assumed to be 0.5 and 1.0. However, some test results revealed the limitation of the ALA

method. The discrepancies between the test results and prediction were believed to arise from the pinching and trench effects.

2.2.2 Numerical Studies

Wijewickreme et al. (2009) used FLAC 2D (explicit finite difference approach) to study the response of soil dilation on the normal stress increase on the pipe. The effect of soil dilation was mimicked by numerically expanding the pipe (0.7 to 1 mm) instead of simulating the pullout directly. The normal stress increase obtained in the numerical model was in good agreement with the experimental observation. The three-dimensional axial pullout of pipe was not directly simulated in their study.

Meideni et al. (2017) used the discrete element method to study the axial pipe-soil response of PVC pipes buried in granular material (Fraser river sand). The maximum axial resistance obtained from the numerical model was found to be higher than the values predicted using the equation suggested in the guidelines. The increase in normal stresses was noticed around the pipe during the pullout. The increase in contact force density was found in the soil zone of 1.5D (1.5 times the diameter of the pipe) radially. Further, they noticed much soil movements in the close vicinity of the pipe, and it incrementally increased toward the pullout direction.

2.3 Finite element modelling

The finite element method is widely used to model complex engineering problems to find the approximate solutions in the computer platform. The finite element approach is supported by several popular computer software packages such as Abaqus, ANSYS and

LS-Dyna. Modelling features related to the pipe-soil interaction problem available in Abaqus software are discussed below as Abaqus is used the FE modelling performed in this study.

2.3.1 Modelling techniques

2.3.1.1 Element types

Abaqus element library contains several solid element types which can be used to model the soil behavior. These include C3D4, C3D8, C3D8R, and C3D20R. Researchers used the C3D8R element, which is an eight-noded linear brick element with hourglass control and reduced integration features, to model the soil behavior successfully (Roy et al. 2015 and Almahakeri et al. 2016). The C3D8R element has 3 active degrees of freedom. Researchers also used C3D20R element, which is a more flexible 20 noded hexahedron element with a reduced integration feature. However, it was reported that analyses performed using this element resulted in convergence difficulties (Almahakeri et al. 2016; Popescu et al. 2001a). C3D8R is an hourglass controlled element which reduces the hourglass effect in the results. Even though this element is a 1^{st} order element, it is a reduced integration element and avoids shear locking in the model.

The Abaqus element library consists of several finite-strain shell elements such as S4R, S3R and SAX1, which can be used to model the problem which involves finite membrane strains and arbitrarily large rotations. To model the pipe and tank behavior involved in the current study, S4R, which is a four-noded general-purpose element, is found most suitable. Almahakeri et al. (2016) reported that S4R elements performs well in large strain analyses. The S4R element has 6 active degrees of freedom and restricts shear and membrane locking

because it is a reduced integration element. This element also has several hourglass modes to lessen the hourglass effect.

2.3.1.2 Nonlinearities

Nonlinearities of a problem can arise due to material nonlinearity, geometric nonlinearity, and boundary conditions nonlinearity. Material nonlinearity is when the stress-strain behavior of the material is non-linear. The pipe and the tank are expected to behave as an elastic material; however, the soil is an elastoplastic material, and can reach the plastic state with very little strain. The Abaqus material library consists of several plastic models such as Tresca, Von Mises, Drucker Prager, and Mohr-Coulomb models. Among those material models, Drucker Prager and Mohr-Coulomb models are suitable to model soil behavior. However, the Mohr-Coulomb model is widely used as a soil model in the previous research (Yimsiri et al. 2004; Guo and Stolle 2005; George et al. 2013; Almahakeri et al. 2016). The details of the built-in Mohr-Coulomb model available in Abaqus are discussed in the next section.

The soil deformation close to the pipe during the pipe pullout is expected to be large. Therefore, geometric nonlinearity should be considered. The geometric nonlinearity of the problem demonstrates the necessity of the nonlinear stiffness matrix. In Abaqus/Explicit, the geometric nonlinearity is automatically incorporated; however, in Abaqus/standard, the geometric nonlinearity should be enabled in the step module. When the geometric nonlinearity presents in the analysis, it is important to set the time increment parameters appropriately.

The major nonlinear boundary condition for this problem is the contact definition. Pipe-soil interface and tank-soil interface are simulated using the built-in surface to surface contact approach available in Abaqus. The surface to surface contact is suitable for the interaction between two deformable bodies or between a deformable body and a rigid body. In this approach, the friction coefficient is used to define penalty based tangential behaviour (Coulomb friction model) and hard contact with separation after contact definitions are used for normal behaviour between interfaces. In general, the value of the friction coefficient (friction factor, *f*) falls in the range of 0.5 to 1.0, depending on the surface roughness. Table 2.1 shows the recommended friction coefficient value in ALA 2001.

Table 2.1 Friction factors for different pipe coatings (ALA 2001)

Pipe coating	*f*
Concrete	1.0
Coal Tar	0.9
Rough Steel	0.8
Smooth Steel	0.7
Fusion Bonded Epoxy	0.6
Polyethylene	0.6

2.3.2 Constitutive modelling of sand

2.3.2.1 Stress–strain behavior of sand

The mechanical response of sand is affected by particle size distribution, grain sizes, specific gravity, and angle of internal friction. The shear strength of sand is distinguished

by the parameter related to interparticle friction (angle of internal friction and critical state friction angle) and volume change (dilation angle). The shear strength of sand interpreted by the following formula (Eq. 2.1), when the cohesion of sand is assumed to be zero.

$$\tau_f = \sigma_f^{'} tan\phi_m^{'} \quad [2.1]$$

here, τ_f is shear stress at failure on the failure plane, $\sigma_f^{'}$ is effective normal stress at failure on the failure plane, and $\phi_m^{'}$ is an effective mobilized friction angle.

Furthermore, researchers identified the significance of dilation of dense sand on the mobilized angle of internal friction (Rowe 1962; Mitchell 1963; Bolton 1986). Bolton (1986) proposed a simple formula (Eq. 2.2) to estimate the mobilized friction angle (ϕ_m') in terms of the critical state friction angle (ϕ_c') and dilation angle (ψ_m).

$$\phi_m^{'} = \phi_c^{'} + 0.8\psi_m \quad [2.2]$$

The stress-displacement behavior of loose sand and dense sand in the triaxial condition is shown in Figure 2.1(a). As noted in the figure, when the strain increases, the dense sand reaches a peak shear stress (measured as the deviatoric stress in the triaxial test) and then drops to a constant stress level. However, stresses in loose sand reach a constant value without showing any peak when it is sheared to the large strain level.

Figure 2.1(b) shows the relationship between volumetric strain and axial strain. The positive side of the vertical axis shows the expansion of soil while the negative side of the vertical axis shows the contraction/compression of the soil. The dense sand initially

contracts and then starts to expand until a constant volumetric strain is reached. Nevertheless, the loose sand continuously contracts until a constant volumetric strain is reached. The gradient of this curve is defined as the dilation angle. It could be noted that the peak shear strength is mobilized when the dilation angle reaches its maximum value.

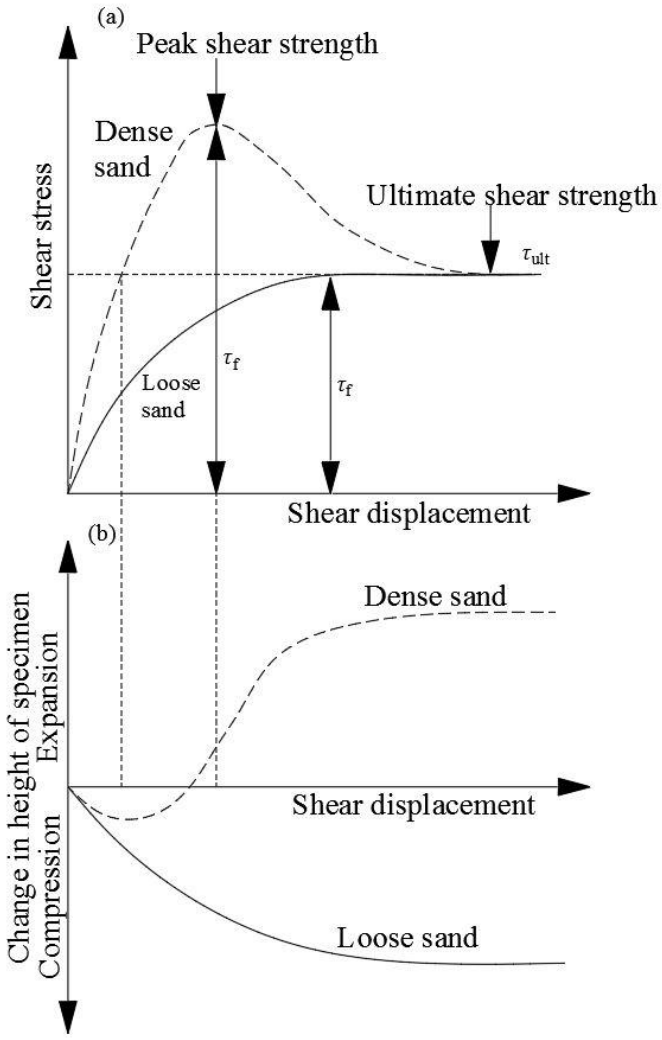

Figure 2.1 Typical drained triaxial test results of dense and loose sand (a) Shear stress versus axial strain (b) Volumetric strain versus axial strain (Das 2008)

2.3.2.2 Mohr-Coulomb model

Selection of an appropriate soil constitutive model is very important in finite element modelling to simulate the realistic behaviour of sand. The Mohr-Coulomb model is one of the in-built material models available in Abaqus to model the soil behavior. Researchers used the Mohr-Coulomb model to idealize the soil response in pipe-soil interaction problems (Yimsiri et al. 2004; Guo and Stolle 2005; George et al. 2013; Almahakeri et al. 2016).

The Mohr-Coulomb (MC) model is an elastic-perfectly plastic model where the soil behaves elastically until the stress state in the soil reaches the failure criteria (Yield surface). Mohr-Coulomb failure criteria can be developed by plotting the Mohr's circle for different stress states at the yield condition (Figure 2.2). The tangent line of these Mohr's circle is defined as the yield or failure line.

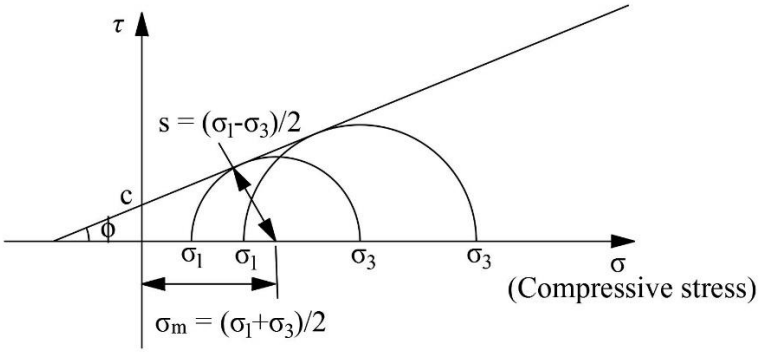

Figure 2.2. Mohr-Coulomb model in Abaqus (Abaqus 2016)

The Mohr-Coulomb model in the deviatoric plane is shown in Figure 2.3. It can be noted that the yield surface depends on the friction angle(ϕ). When $\phi = 0°$, yield surface is

considered a Tresca model. When the $\phi = 90°$, the yield surface is considered a Rankin surface. The plastic flow rule in the deviatoric plane is "non-associated".

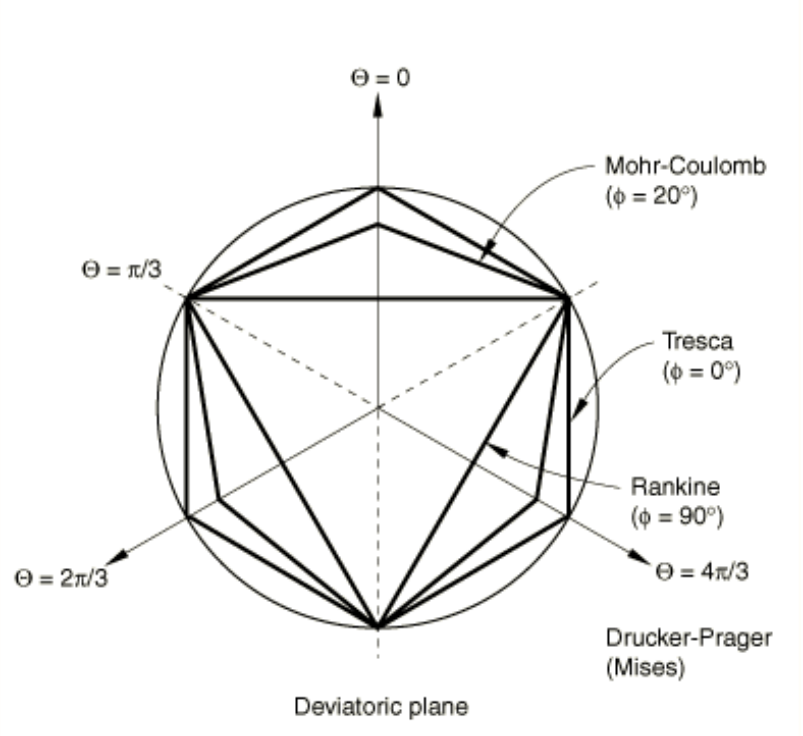

Figure 2.3. Mohr-Coulomb yield surface in the deviatoric plane (Abaqus 2016)

In this model, when the soil stresses reach the failure (yield) surface, plastic strains are developed in the soil, and the soil dilates at the constant dilation angle. The soil behavior in actuality has small differences because plastic strains are developed in the soil even before it fails, and the soil dilation is not constant. However, the MC model could be successfully used to estimate the ultimate soil resistance during the pipe pullout simulation. Yimsiri et al. (2004) showed that the MC model gives reasonable response during the pipe-soil interaction simulation. The parameters required to define the MC model are Young's Modulus (E), Poisson's ratio (ν), the angle of internal friction (ϕ'), dilation angle (ψ_m), and

unit weight of soil (γ). The dilation angle is a constant value in the built-in MC model in Abaqus.

To model the ductile iron pipe and test cell wall behavior, elastic properties of steel are sufficient since the elastic response of the pipe and test cell wall is focused in this study.

2.5 Summary

A summary of existing experimental and numerical studies on the axial pullout of buried pipelines, and different finite element modelling techniques related to the pipe–soil interaction problem are discussed in this chapter. Researchers identified the increase in normal stress around the pipe during the experimental investigations conducted in dense sand. The comparison of pullout resistances obtained from the tests with the ALA (2001) method showed that the ALA method underpredicts the soil resistance for dense sand condition, whereas ALA method gives a close estimation for loose sand. This is attributed to the incorrect calculation of normal stress at the pipe-soil interface. For numerical modelling, the default Mohr-Coulomb material model available in Abaqus was identified as a reasonable soil material model which can be used in the pipe-soil interaction problem. However, the effect of strain hardening and softening of soil could not be simulated using the Mohr-Coulomb model. Although a few experimental and numerical studies on axial pullout behavior of steel pipes are available in the literature, studies using ductile iron pipe are limited and still require extensive investigations.

CHAPTER 3

A Laboratory Facility for Studying Pullout Behavior of Buried Pipelines

Co-Authorship: This chapter has been published as a technical paper in the 71st Canadian Geotechnical Conference and 13th Joint CGS/IAH-CNC Groundwater Conference as Murugathasan, P., Dhar, A. and Hawlader, B. 2018. 'A laboratory facility for studying pullout behaviour of buried pipelines.' Most of the research in this chapter has been conducted by the first author under the supervision of Dr. Ashutosh Dhar. The draft of the manuscript is also prepared by the first author with the guidance of Dr. Ashutosh Dhar. The other authors supervised the research and reviewed the manuscript.

3.1 Abstract

The effect of ground movements on the performance of buried pipelines is an important consideration for pipeline integrity assessment. The experimental and analytical studies conducted in the past identified the important shearing mechanisms of soil around the pipe during relative ground movements. However, design methods for the assessment of pipes subjected to ground movements are not well developed, due to the lack of quantitative data on the effects of soil shearing on the pullout force of the pipeline. The objective of the current study is to develop a laboratory test facility for pullout testing of buried pipelines to investigate pipe with different diameters and materials while simulating the ground conditions expected in the field. Finite-element modelling is used to assess the effects of the size of the test facility and rigidity of the boundary wall on the pullout behaviour. Based on the calculated effects, an optimum design of the test box is developed. The findings from

this study suggest that a width of 10 times pipe diameter for the test cell is sufficient for axial pullout testing; however, the boundary wall stiffness should be designed to adequately minimize the wall deformations.

3.2 Introduction

Buried pipelines have increasingly become the most popular transportation media of water and hydrocarbons, in recent years. Although buried pipelines are accepted as safe and feasible transporting media around the world, they face a major challenge when any ground movements occur due to landslides. The resulting relative ground movements generate external forces on pipelines in a longitudinal, transverse or oblique directions depending on pipe orientation against ground movements. Researchers employed laboratory pullout tests to investigate the ground loads on pipelines subjected to ground movements (e.g., Paulin et a. 1998, Wijewickreme et al. 2009, Daiyan et al. 2011). The main objective of this research is to develop a full-scale laboratory test facility which will be used to study the pullout behaviour of buried pipelines.

In the development of a test facility, the boundary wall effects are major constraints that can affect the test results considerably. Available experimental test data on pullout behaviour of buried pipelines are limited to particular pipe diameters/materials and often not comprehensive enough to address the effect of soil shearing during the pipe pullout. Numerical and analytical studies in this area still require more accurate data for validation/calibration purposes. For this reason, the focus of this study is to design a test facility which can be used to study pullout behaviour of pipe with different sizes.

This chapter presents the results of finite-element analyses that have been conducted to examine the effect of test cell size and its wall rigidity while testing for pullout behaviour of buried pipelines. Numbers of finite-element models are analyzed to assess a suitable cell size and stiffness of cell wall to limit displacement of the side boundary walls due to soil pressure generated during backfilling of soil and pullout testing. Initial stresses of soil and shear-induced expansion of soil are simulated subsequently by considering gravity load and expanding the pipe boundary numerically.

3.3 Review of Previous Studies on Laboratory Test Facility

Several full-scale experimental studies were conducted in the past to investigate pipe-soil interaction behaviour when the buried pipe is subjected to longitudinal or transverse movements. However, the number of laboratory tests conducted for modelling axial pullout behaviour of buried pipe is still limited. Paulin et al. (1998) developed a full-scale test facility which was constructed using concrete block walls. The test facility was adjustable to two different testbed configurations with dimensions of 3 m (width) × 1.4 m (height) × 3 m (length) and 0.63 m (width) × 1.4 m (height) × 5.2 m (length) for lateral and axial tests, respectively, to study force–displacement behavior of pipeline buried in sand and clay soils. Soil movements and vertical deformation profiles of the test bed during the pipe movement were monitored. The axial pullout tests conducted in clay soil showed that the displacement required to mobilize maximum resistance was much less than the suggested values in ASCE (1984). The comparison of the back-calculated adhesion factor using the test results showed that the adhesion values are over-predicted in the existing design codes. Alam and Allouche (2010) used a 1.83 m (width) × 1.83 m (height) × 3.66 m (length) steel soil chamber with a

0.6 m high lid on top to assess the friction coefficient of the pipe-soil interface when the pipe is axially displaced. Axial tensile load tests on PVC pipes with an internal diameter of 203.2 mm were conducted for a range of different soil types. The inner walls of the chamber were covered by three layers of polythene sheets with lubricant applied between the layers to reduce the wall friction. Elongation of the pipe, rigid body movement of the pipe, applied load and earth pressures around the pipe were measured during the axial pulling of the pipe. The earth pressure measurement showed a sudden drop at the crown of the pipe. The measured earth pressure close to the pipe near the springline showed an increase while the measurements at 450 mm away from the pipe showed fairly constant earth pressures during the movement of the pipe. The effects of boundary conditions were not assessed exclusively in detail in this study. Wang and Yang (2016) conducted full-scale testing on 172.3 mm and 223.1 mm diameter steel pipes buried in soft clay using a 1.4 m (width) × 1.0 m (height) × 1.5 m (length) test chamber in order to determine the axial friction coefficient (adhesion factor) of the pipe-soil interface. The boundary effect on the adhesion factor was reported to be negligible for the tests in the test chamber. Wijewickreme et al. (2009) performed full-scale tests to investigate the axial pipe-soil interaction of buried pipelines which were subjected to an axial pullout force. They examined the variation of normal soil stresses on the pipe surface to investigate the influence of dilation of sand due to shearing near the pipe-soil interface. The test facility was made of a timber frame with the dimensions of 2.5 m (width) × 2.5 m (height) × 3.8 m to 5 m (length). The axial pullout tests were performed using a 457 mm diameter steel pipe buried in a loose/dense state of Fraser river sand at H/D (depth to diameter) ratios equal to 2.5 and 2.7. The computer program FLAC 2D, which

was developed based on a two-dimensional (2-D) explicit finite difference method, was used to assess the effects of the boundary distance of the longer walls. It was reported that the soil stresses had no significant changes near the boundary walls during the pullout test. Further, it was observed that the length of the test chamber had no significant effect on pipe pullout behaviour based on the tests conducted with two different test chamber lengths. They applied radial expansions of 0.7 to 1 mm in the pipe-soil interface for their numerical simulation to simulate soil dilation during shearing when the pipe is pulled. Karimian (2006) reported that only 1.2 to 2.8 mm of sand thickness is sheared during pipe pullout based on their tests conducted on sand-blasted steel pipes and polyethylene pipes buried in Fraser river sand.

Several full-scale lateral pullout tests were also performed to investigate the force–displacement behaviour of buried pipelines. Trautmann et al. (1985) tested lateral and uplift behaviour of buried pipe in dry Cornell filter sand to study the force–displacement relationship of different soil densities using various H/D ratios. 1.2 m (width) × 1.2 m (height) × 2.3 m (length) and 1.22 m (width) × 1.52 m (height) × 2.29 m (length) test boxes made of plywood were used for lateral and uplift tests, respectively. The chamber walls were further stiffened using lumber ribs to reduce the deflection of the side walls. The lateral tests were conducted using 102-mm and 324-mm diameter steel pipes and the uplift tests used 102-mm diameter steel pipes. Almahakeri et al. (2016) used a full-scale test facility which was surrounded by retaining walls with the inner dimension of 2 m (width) × 2 m (height) × 3.01 m (length) to investigate the bending behaviour of glass-fiber reinforced polymer (GFRP) pipes when subjected to lateral movements. They used 102 mm

diameter steel and GFRP pipes with 3 different depth to diameter ratios to study the problem. The force–displacement data, deflection of pipe, strain on the pipe's outer surface and soil surface deformations were measured. Robert et al. (2016b) investigated the effects of unsaturated states of soils on pipe–soil interaction based on two different sands with laterally loaded pipe. The tests were conducted in Chiba sand and Cornell sand using two different test facilities and different laboratories. A 3.0 m (width) × 2.03 m (height) × 2.02 m (length) tank with a steel frame was used to test a 114.6 mm diameter steel pipe buried in Chiba sand at H/D = 6, and a 2.4 m (width) × 1.8 m (height) × 2.4 m (length) steel frame test box was used for the Cornell sand test. Pipe displacements in the horizontal and vertical directions and the earth pressure variations were measured during the test. Wang et al. (2017) investigated soil–nail interaction during pressure grouting using a steel soil chamber which had an internal dimension of 0.6 m (width) × 0.73 m (height) × 1 m (length). The side walls of the tank were made using a 10 mm thick steel plate with square steel stiffeners. A lubricant was applied between a flexible plastic sheet and stainless-steel wall to reduce the friction of the tank wall. Applied force, resulted displacement and earth pressures around the nail were measured during the tests. The applied force was measured using a reaction frame with a hollow jack and a load cell when the nail was pulled with a controlled displacement rate. Robert et al. (2016a) used another 3.2 m (width) × 2.3 m (height) × 10.5 m (length) test box made of a steel frame and tested a 400 mm diameter HDPE pipe buried in glaciofluvial sand (Cornell sand) at 1.12 m depth to investigate the pipeline behaviour subjected to fault movement. The test box was split into two units in a way that enabled each unit to slide relatively at an angle of 65°.

In addition, centrifuge tests have been reported on studying the transverse or oblique movement of buried pipes (Ha et al. 2008; Daiyan et al. 2011; Dickin 1994). Also, numerical studies were performed on pipe-soil interaction (Phillips et al. 2004; Yimsiri et al. 2004; Pike and Kenny 2012; Almahakeri et al. 2016) with pipes subjected to different modes of movements.

3.4 Design of Test Cell

A test cell with dimensions of 2 m (width) × 1.5 m (height) × 4 m (length) is first considered. These dimensions provide a width of 20 times the pipe diameter and a height of 15 times the pipe diameter for a 100 mm diameter pipe. The schematic drawing of the cross-section of the cell is shown in Figure 3.1. A pipe diameter of 100 mm buried at the H/D ratio of 6 is investigated for the effects of the test cell boundaries during pullout tests. The side-wall distance and bedding distance are 10D and 6D, respectively, in the first model. However, different wall distances are considered to assess the boundary effects and the results are discussed later in this chapter. The overall size of the cell is optimized to make the laboratory testing more convenient while ensuring sufficient boundary distances.

Type A36 steel is selected for the test cell, which is readily available material. A36 steel has a density of 7850kg/m3, Young's modulus of 200GPa, and a minimum yield strength of 250MPa (American institute of steel construction 1986). The thickness of the test cell wall is selected as 6 mm and is kept unchanged in the design to maintain a reasonable overall test cell weight. The rigidity of the boundary walls is increased by adding stiffeners

to the wall, instead of changing the wall thickness and material. The steel plates are stiffened by adding more longitudinal and transverse stiffeners outside of the cell wall.

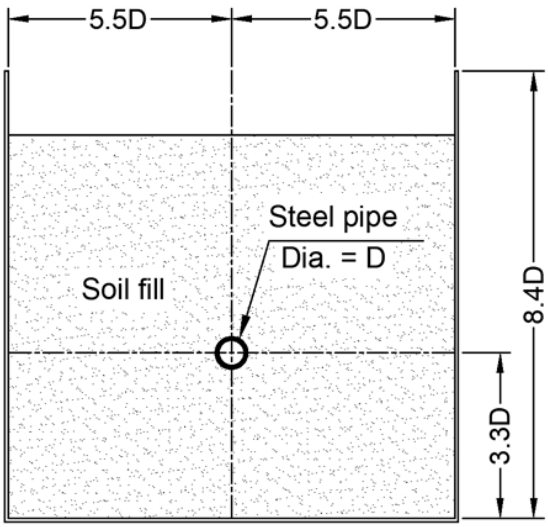

Figure 3.1. Schematic drawing of test cell's cross-section

In addition to adequate cell size and wall rigidity requirements, some special features are planned into the test chamber to make the test chamber more versatile. Polycarbonate sheet (Lexan) window panels are planned in the chamber wall to facilitate observations inside the chamber (30 cm wide and 130 cm deep panels). However, this has not been considered in FE modelling presented here. Circular openings are considered in the model on the front and back walls, enabling running a longer pipe through the chamber or fixing a hydraulic actuator to the pipe. Lubricated polyethylene sheets are used to reduce the cell-wall interface friction. Tognon et al. (1999) obtained the cell-soil interface friction angle of less than 5° using lubricated polymer sheets.

3.5 Numerical Modelling

3.5.1 Modelling Approach

The numerical analysis is conducted to investigate the appropriate boundary distances and wall rigidity of the test facility which is to be developed for axial pullout testing of buried pipelines. The numerical modelling is carried out using the commercially available finite-element software package Abaqus/Explicit. The large deformation of the soil and test cell wall due to the gravity load (soil fill) and the contact definitions between two deformable bodies demonstrate the necessity of using explicit finite-element code for this analysis. Two-dimensional plane strain analysis is first carried out to assess the effect of boundary wall distance and wall friction on the pipe-soil interface behaviour. However, actual cell wall rigidity and boundary restraints could not be simulated properly in the 2-D model. Therefore, a three-dimensional (3-D) continuum-based model is developed at the same scale as the proposed experimental facility of pullout testing to investigate the effect of boundary wall rigidity on the longitudinal pipe movements. In the 2-D model, the soil and pipe are modelled using a four-noded linear quadrilateral element (CPE4R). The tank wall is modelled using the beam element (B21) which is a two-noded linear beam element in a plane. The typical finite-element mesh used in the 2-D analyses is shown in Figure 3.2.

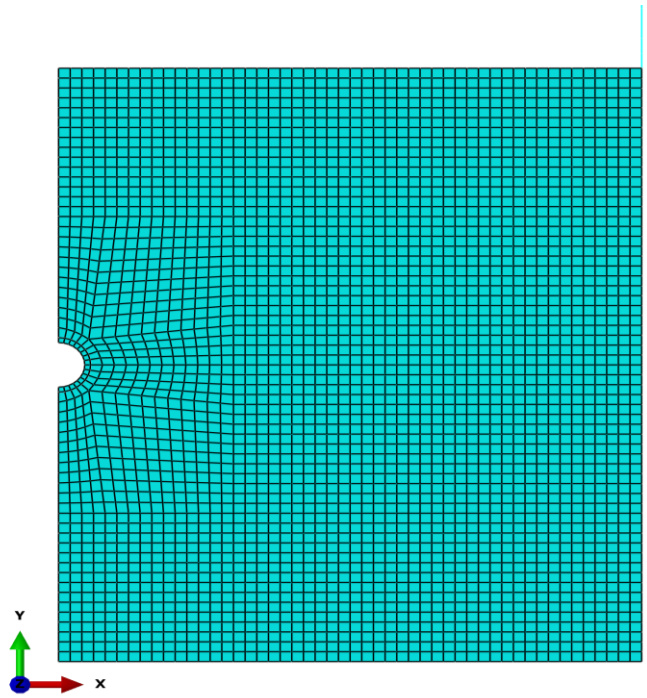

Figure 3.2. Typical finite-element mesh of soil, test cell and pipe used in 2-D model

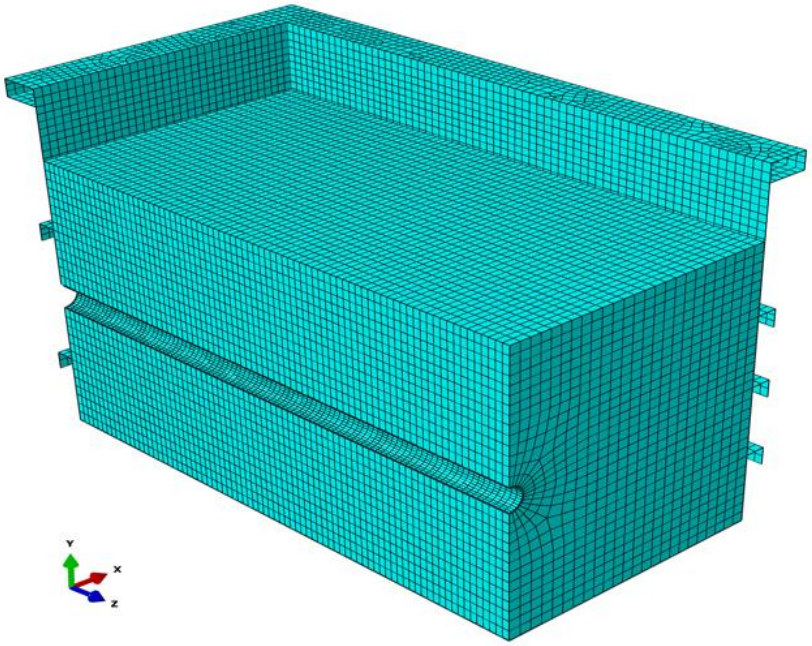

Figure 3.3. Typical finite-element mesh of soil, test cell and pipe used in 3-D model

In the 3-D model, the soil is modelled as continuum material using an eight-noded linear brick element (C3D8R). The cell wall and pipe are modelled using four-noded 3-D doubly curved shell elements (S4R). The typical finite-element mesh used in the 3-D analyses is shown in Figure 3.3. Suitability of the beam element and shell element is first assessed to select an effective element type to model the stiffeners. The use of shell elements with small mesh size has shown similar bending stiffness as beam elements do. Furthermore, avoiding the constraints between the beam and shell elements reduces the computational time significantly. Thus, the shell element (S4R) is employed for the stiffeners. The use of hourglass controlled elements (C3D8R, CPE4R & S4R) reduced the effects of hourglass modes in the results. Even though these element types are 1st order elements, as these are reduced integration elements, shear locking of elements is automatically avoided in the model response.

Mesh convergence analysis and element quality assessment are conducted separately to make sure that analysis results are independent of the mesh size and mesh quality for each model. A structured mesh has been generated for soil, pipe, and cell with denser mesh near the pipe.

3.5.2 Boundary Conditions and Loadings

The pipe-soil interface and cell-soil interface are simulated using the built-in surface to surface contact approach available in Abaqus. In this approach, the friction coefficient is used to define the tangential behaviour (penalty type), and hard contact with separation after contact definition is used for normal behaviour between the surfaces. In this method,

if the shear stress on the contact interface exceeds the critical shear stress (friction coefficient times normal stress), sliding occurs.

In addition to the nonlinear contact boundary conditions, the bottom face of the test tank is restrained for rotation and displacement in x, y and z directions. The vertical faces of the tank are not restrained in any direction; rather, walls are allowed to deform based on their flexural rigidity. Due to symmetrical geometry and loading conditions, only one-fourth and half of the physical model is created for the 3-D and 2-D analysis, respectively. Appropriate symmetric boundary conditions on the symmetric planes are employed.

The finite-element analysis is conducted in two main steps. The first step is to apply the gravity load that accounts for the effects of soil weight and creates the initial stresses on the soil. Besides developing initial soil stress, this step is quite important to assess the boundary wall deformations and corresponding changes in the soil stresses. The coefficient of lateral earth pressure under this condition is examined and is found to be close to the K_0 condition calculated using the elastic theory ($\nu/(1-\nu)$). In the second step, the pipe is enlarged by 1 mm (after, Wijewickreme et al. 2009) to mimic the effect of the shear-induced expansion of soil in the pipe-soil interface during the pullout.

3.5.3 Material Model and Parameters

The built-in Mohr–Coulomb model in Abaqus is used to model the soil. The Mohr–Coulomb model requires the following input parameters: Young's Modulus (E), Poisson's ratio (ν), the angle of internal friction (ϕ'), dilation angle (ψ_m) and unit weight of soil (γ). Good representative typical values of soil parameters are chosen for this analysis. A dilation

angle of 5° is estimated by considering a peak friction angle of 35° and the critical state friction angle of 31°, based upon the relationship proposed by Bolton (1986). As the steel stresses are to be limited to the elastic region, only the elastic properties of steel are employed, and the plastic behaviour of steel is not modelled. The test cell and pipe are assigned with the same steel properties. The parameters used in the FE model are summarized in Table 3.1.

Table 3.1. Parameters used in FE analyses (design of test cell)

Parameter	Value
E_{soil} (MPa)	10
ν_{soil}	0.25
ϕ' (°)	35
ψ_m (°)	5
Density of soil, ρ_{soil} (kg/m^3)	1700
Cohesion[a], c' (kN/m^2)	0.1
E_{steel} (GPa)	200
ν_{steel}	0.3
Yield strength, σ_{y} (MPa)	250
Density of steel, ρ_{steel} (kg/m^3)	7850

[a]A small value of cohesion is assumed to model the Mohr–Coulomb model in Abaqus for numerical stability.

The friction coefficient (μ=tan (ϕ_μ)) is estimated in terms of interface friction angle (ϕ_μ). The interface friction angle, ϕ_μ, depends on the interface characteristics and the degree of relative movement between the two surfaces. A constant value of, μ = 0.3 is employed for the pipe-soil interface in this study. However, different friction coefficient values are used for the cell-soil interface to assess its effects on the soil response.

3.6 Results and Discussion

3.6.1 Preliminary Analyses

Several different wall thicknesses of the test cell are considered to investigate the effect of boundary wall rigidity on the initial soil stress development in the test cell and on the dilation (expansion of dense soil during axial pipe movement) using the 2-D plane strain analysis. Self-weights of the soil (γH) and the pipe are used to develop initial stresses in the soil domain. The additional surcharge load could be simulated by considering a higher fill of soil above the pipe but it is not exclusively considered in this study; rather, a constant H/D ratio is employed to study the boundary effect. The coefficient of lateral earth pressure at-rest (K_0) is not directly employed in the model. Therefore, the lateral earth stresses expected in the field should be developed by limiting the outward deformation of the cell wall. In order to achieve this, the cell wall should be sufficiently rigid. Ultimately, a steel plate having a thickness of 100 mm shows more rigid behavior with approximately zero lateral deformation of the wall and gives a reasonable initial vertical and lateral soil stress profile, as expected in the field. A cell–soil friction angle of 5° is employed in this model. The effect of cell-soil interface friction angle on the initial soil stress development and on the simulation of soil dilation at the pipe-soil interface is studied separately using the 2-D

model with the dimensions of 2 m (width) x 1.5 m (height). Figure 3.4 shows the variation of calculated vertical soil stresses near the boundary wall with depths for different cell-soil interface friction angles of 1°, 5°, 10° and 15°. The developed vertical soil stresses decrease with depth when the cell-soil interface friction angle increases due to the shear stress developed along the wall. However, it is also noted that initial vertical and horizontal stresses near the pipe are not much affected by the wall friction angle when the wall is rigid and far enough from the pipe. Figure 3.5 shows the calculated vertical soil stresses near the pipe (0.2 m away from pipe center) with depth (between 0.3 m and 0.9 m soil depth) for cell-soil interface friction angles of 1° and 15° during the dilation simulation of the pipe pullout step. It clearly shows that the effect is insignificant at mid-depth although a small variation of the calculated vertical stress is observed at greater soil depth. The effect of friction angle is found to be significant if the cell wall is close to the pipe.

3.6.2 Effect of Wall Distance and Wall Rigidity on the Soil Response

The results of the 2-D and 3-D models are used to examine the effects of wall distance and wall rigidity during the gravity step and during the simulation of soil dilation with the pipe pullout step. The cell-soil interface friction angle of 5° is used. The 3-D models are developed with the dimensions of a 2 m (width) x 1.5 m (height) x 4 m (length) and 6 mm thick wall, but with a different configuration of stiffeners until the wall deformations are controlled. Channel sections of 150 mm x 75 mm x 10 mm size are used for horizontal stiffeners at the top of the cell. Angle sections of 75 mm x 75 mm x 10 mm size are used to model all other stiffeners. Vertical stiffeners are used at approximately 0.5 m intervals. This facilitates the side wall displacement of the test cell to be within 1 mm after the gravity

step and after the simulation of soil dilation. The results are shown in Figures 3.6 and 3.7, respectively.

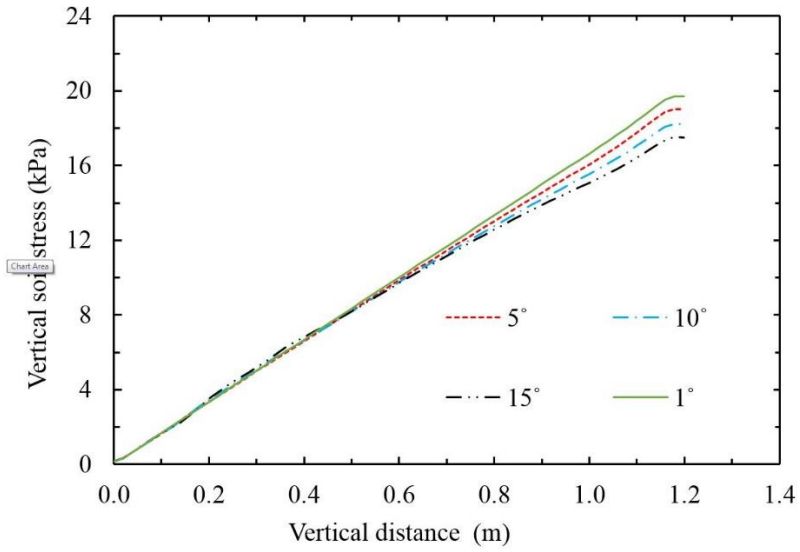

Figure 3.4. Vertical stresses with soil depth, 0.2 m away from the cell wall (initial loading)

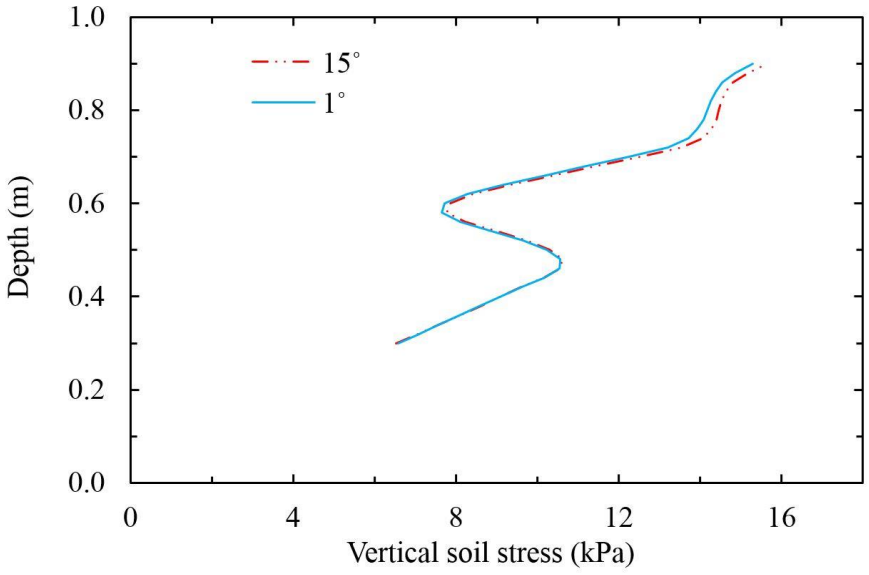

Figure 3.5. Vertical stresses with soil depth, 0.2 m away from the pipe centre during expansion

A maximum horizontal displacement of 0.27 mm occurs on the lateral walls at the end of the gravity step (Figure 3.6). Subsequently, the wall displacement has increased only by 0.29 mm when the pipe is numerically expanded by 1 mm in the second step (Figure 3.7). The initial vertical and horizontal soil stresses are developed after the application of gravity load, as expected; however, they are not exactly same as the results of the 2-D model, due to comparably less wall rigidity in the 3-D model, as discussed below. Since the increase in wall deformation is negligible in the second step, it is assumed that the soil dilation around the pipe would not be significantly influenced by the boundary of the cell.

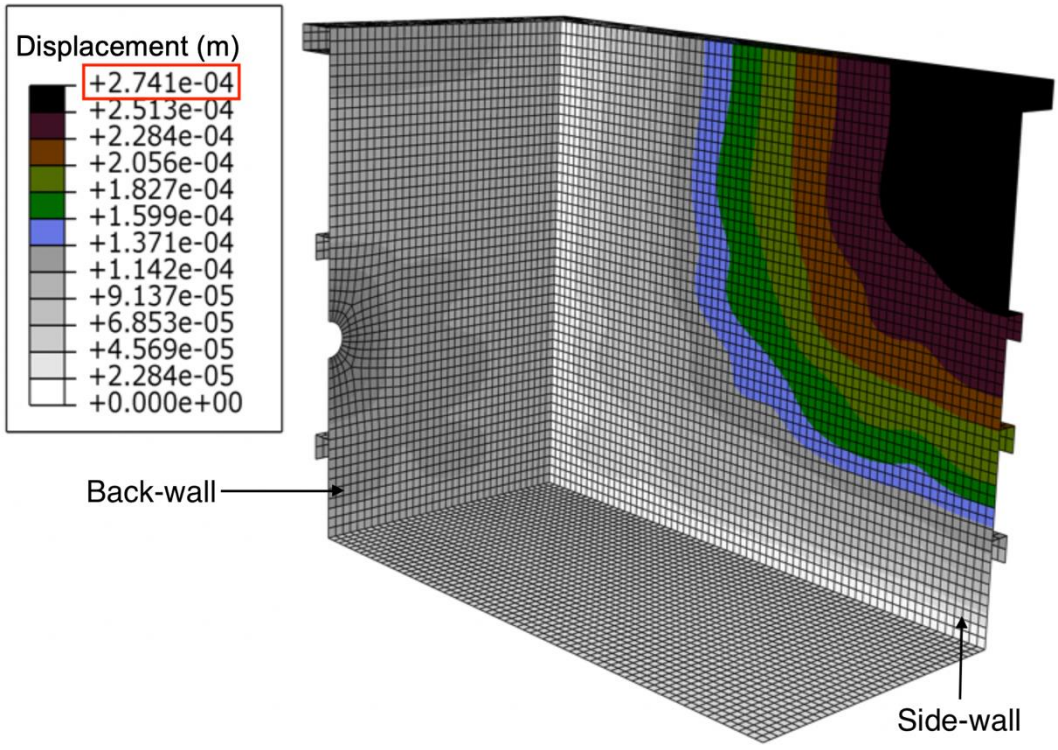

Figure 3.6. Deformation of test cell after gravity step

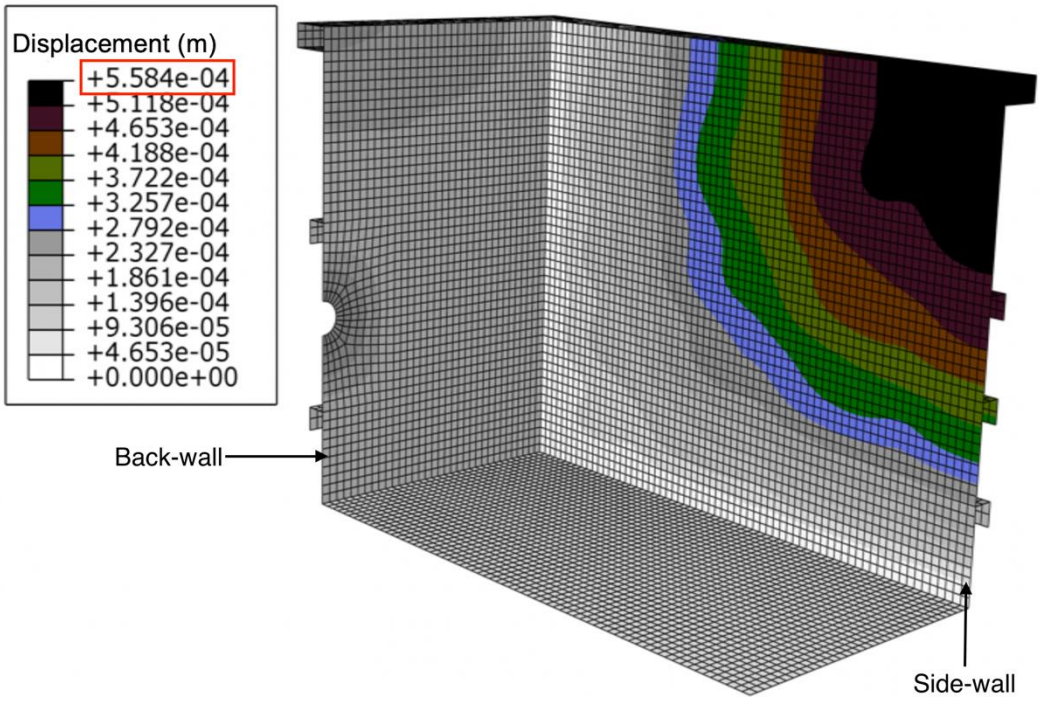

Figure 3.7. Deformation of test cell after simulation of dilation during the pullout

The vertical and horizontal soil stresses at the springline level are examined to investigate the boundary effect on the pipe-soil response during the simulation. The results in Figure 3.8 show the variation of calculated horizontal stresses along with the springline level at the end of the initial soil stress development step and after 1 mm expansion of the pipe for both 2-D and 3-D models. Both 2-D and 3-D models generate very close soil stresses in the initial gravity step. The horizontal soil stresses are increased significantly around the pipe in the second step and decrease towards the boundary wall. However, the increase in horizontal soil stresses in the 3-D model is less than the stress developed in the 2-D model. This difference could be due to low wall rigidly in the 3-D model. Moreover, it is noted that the soil stress change near the cell wall is only about 7.5% of the soil stress

change near the pipe (i.e. stress increase near the pipe is 27 kPa, whereas the increase near the cell wall is 2 kPa, based on the 3-D model).

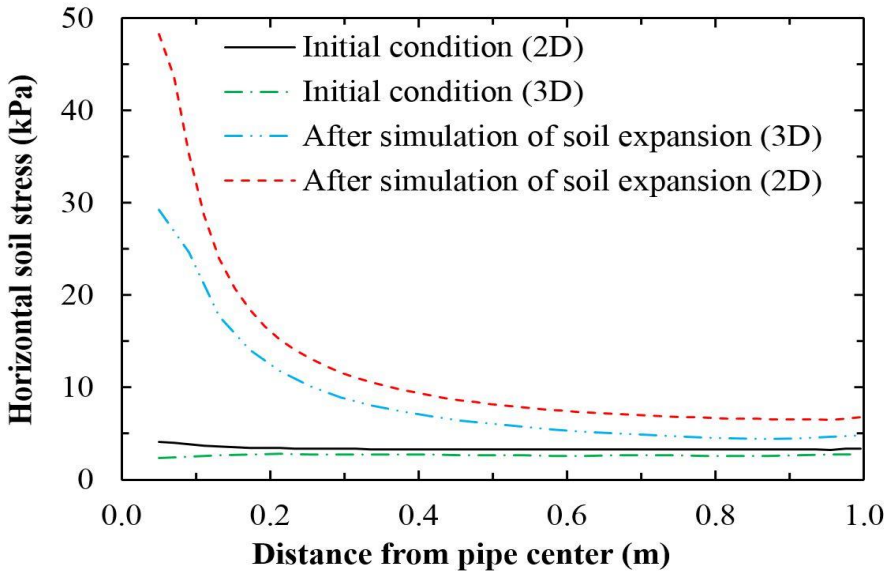

Figure 3.8. Horizontal soil stresses at springline level from pipe centre to cell wall

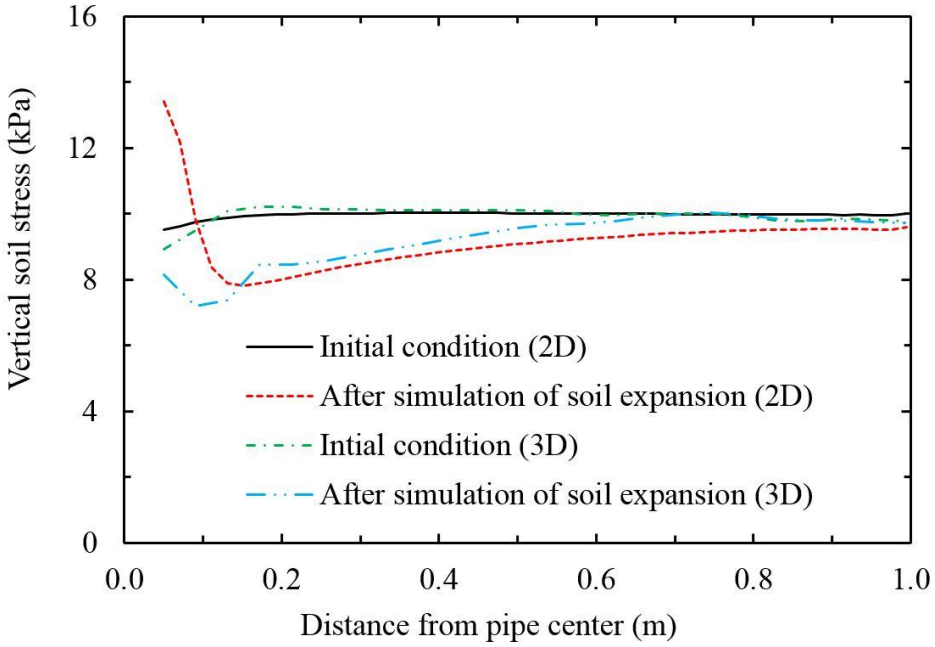

Figure 3.9. Vertical soil stresses at springline level from pipe center to the cell wall

Figure 3.9 shows the distribution of vertical soil stresses along the springline level for both 2-D and 3-D models at the end of two loading steps. Both models show a similar soil stress distribution in both steps. However, the 2-D model shows a high vertical soil stress immediately next to the pipe when the pipe is expanded, while the 3-D model shows a lower vertical stress. The soil movements in lateral and longitudinal directions may be the cause of lower stress in the 3-D model. The change in vertical soil stress decreases with the distance and the stress reaches very close to the initial condition towards the boundary wall. Based on the 3-D model results, it is noted that the significant soil stress changes occur within 0.7 m distance from the pipe center when the dilation of the soil is simulated by 1 mm of expansion. In addition, several two-dimensional models with different wall distances are considered to examine the side wall effect on the soil response during the simulation of the soil dilation step. The outcomes demonstrate that a distance of 1 (10D) m is good enough to reduce the boundary effects. Therefore, a 2 m width of the test cell is considered adequate for pipe pullout tests.

3.7 Summary

In this study, a series of finite-element models is employed to develop an optimum test cell size with wall stiffeners for axial pullout testing of buried pipes while developing reasonably similar soil stresses expected in the field. An initial cell dimension of 2 m (width) × 1.5 m (height) × 4 m (length) is used as a base size of the test cell and subsequently, the effects of wall distances and wall stiffeners are studied by changing the width and the stiffener configurations. The analyses are conducted at the H/D ratio of 6 using a pipe diameter of 100 mm. The simple Mohr–Coulomb model is employed to

simulate the soil behaviour. The effect of side wall distance, wall friction and wall rigidity are investigated using both 2-D and 3-D finite-element analyses. The effect of different H/D ratios is not considered in this investigation; rather, a constant H/D ratio is used in all the models. The soil shearing in the pipe-soil interface due to pipe pullout is not directly simulated; instead, it is imitated by expanding the pipe by 1 mm, based upon the values reported in the literature.

The wall rigidity of the cell wall should be adequately designed to control the lateral deformation; otherwise, the resulting movement of soil in the lateral direction could affect the stress distribution in the soil. Higher wall rigidity could be efficiently achieved by adding more stiffeners to the thinner wall instead of increasing the wall thickness. The side-wall distance is another key parameter which should be decided in such a way that the effect due to pipe-soil interface response does not reach the side-wall during the pulling operation. This study suggests that the wall distance of 10D (10 times pipe diameter) is sufficient to eliminate the boundary effects; however, it depends on the amount of sand dilation occurring in the pipe-soil interface. The cell-soil interface friction angle shows a moderate effect on the soil response unless it is limited to lower values. A lower interface friction angle could be achieved by covering the cell inner face with lubricated polyethylene sheets.

Acknowledgments

The authors gratefully acknowledge the financial support for this research provided by the National Science and Engineering Research Council of Canada through its Collaborative Research and Development Grants and FortisBC Energy Inc.

Notation

2-D	two dimensional
3-D	three dimensional
FE	finite element
HDPE	high density polyethylene pipe
D	external diameter of the pipe
E	Young's modulus
H	distance of pipe center from soil surface
K_0	at-rest lateral earth pressure coefficient
ϕ_μ	interface friction angle
γ	unit weight of soil
μ	friction coefficient
ν	Poisson's ratio
ϕ'	angle of internal friction of soil
ϕ'_{cv}	critical state friction angle
ϕ'_{peak}	peak friction angle
ψ_m	maximum dilation angle

References

Alam, S. and Alloche, E.N. 2010. Experimental investigation of pipe soil friction coefficients for direct buried PVC pipes, Pipeline Division Specialty Conference 2010, ASCE, Keystone, Colorado, USA, 2: 1160–1169.

Almahakeri, M., Moore, I., and Fam, A. 2016. Numerical study of longitudinal bending in buried GFRP pipes subjected to lateral earth movements, Journal of Pipeline Systems Engineering and Practice, **8**(1): 702–710.

Bolton, M.D. 1986. The strength and dilatancy of sands, Géotechnique, 36(1): 65–78.

Brachman, R.W., Moore, I.D., and Rowe, R.K. 2000. The design of a laboratory facility for evaluating the structural response of small-diameter buried pipes, Canadian Geotechnical Journal, **37**(2):281–295.

Daiyan, N., Kenny, S., Phillips, P., and Popescu, R. 2011. Investigating pipeline-soil interaction under axial-lateral relative movements in sand, Canadian Geotechnical Journal, **48**(11): 1683-1695.

Dickin, E. 1994. Uplift resistance of buried pipelines in sand. Soils and Foundations, **34**(2): 41–48.

Ha, D., Abdoun, T.H., O'Rourke, M.J., Symans, M.D., O'Rourke, T.D., Palmer, M.C. and Stewart, H.E. 2008. Buried high-density polyethylene pipelines subjected to normal and

strike-slip faulting — a centrifuge investigation, Canadian Geotechnical Journal, **45** (12): 1733–1742.

Karimian, H. 2006. Response of buried steel pipelines subjected to longitudinal and transverse ground movement, Ph.D. thesis, Department of Civil Engineering, The University of British Columbia, Vancouver, B.C.

Paulin, M. J., Phillips R., Clark J. I., Trigg A. and Konuk I.1998. A full-scale investigation into pipeline/soil interaction, International pipeline conference ’98, ASME, Calgary, Alberta, Canada, 2: 779–788.

Phillips, R., Nobahar, A. and Zhou, J. 2004. Combined Axial and Lateral Pipe-Soil Interaction Relationships, International Pipeline Conference IPC2004, ASME, Calgary, Alberta, Canada, 1, 2, and 3: 299–303.

Pike, K. and Kenny, S. 2012. Lateral-Axial Pipe/Soil Interaction Events: Numerical Modelling Trends and Technical Issues, International Pipeline Conference IPC2012, ASME, Calgary, Alberta, Canada, 4: 1–6.

Robert, D., Soga, K. and O'Rourke, T. 2016a. Pipelines subjected to fault movement in dry and unsaturated soils, International Journal of Geomechanics, **16**(5): C4016001-1–16.

Robert, D., Soga, K., O'Rourke, T. and Sakanoue, T. 2016b. Lateral load-displacement behaviour of pipelines in unsaturated sands, Journal of Geotechnical and Geoenvironmental Engineering, **142**(11): 04016060-1–13.

Steel Construction Manual, 8th Edition, second revised edition, American Institute of Steel Construction, 1986, Ch. 1 pp. 1–5

Trautmann, C. H. and O'Rouke, T. D. 1985. Lateral force- displacement response of buried pipe, Journal of Geotechnical Engineering, ASCE, **111**(9): 1077-1092.

Trautmann, C. H., O'Rourfce, T. D. and Kulhawy, F. H. 1985. Uplift force- displacement response of buried pipe, Journal of Geotechnical Engineering, **111**(9): 1061–1076.

Tognon, A.R., Rowe, R.K., and Brachman, R.W.I. 1999. Evaluation of sidewall friction for a buried pipe testing facility, Geotextiles and Geomembranes, 17: 193–212.

Yimsiri, S., Soga, K.., Yoshizaki, K., Dasari, G. R. and O'Rourke T. D. 2004. Lateral and Upward Soil-Pipeline Interactions in Sand for Deep Embedment Conditions, Journal of Geotechnical and Geoenvironmental Engineering, **130**(8): 830-842.

Wang, J. and Yang, Z. 2016. Axial friction response of full- scale pipes in soft clays. Applied Ocean Research, 59: 10–23.

Wang, Q., Ye, X., Wang, S., Sloan, S. W., and Sheng, D. 2017. Experimental investigation of compaction-grouted soil nails. Canadian Geotechnical Journal, **54**(12): 1728–1738.

Wijewickreme, D., Karimian, H., and Honegger, D. 2009. Response of buried steel pipelines subjected to relative axial soil movement, Canadian Geotechnical Journal, **46**(7): 735–752.

CHAPTER 4

An Experimental and Numerical Investigation of Pullout Behavior of Buried Ductile Iron Water Pipes

Co-Authorship: This chapter has been submitted to the Canadian Journal of Civil engineering as a technical paper for review as: Murugathasan, P., Dhar, A. and Hawlader, B. 2019. 'An Experimental and Numerical Investigation of Pullout Behavior of Buried Ductile Iron Water Pipes.' Most of the research in this chapter has been conducted by the first author under the supervision of Dr. Ashutosh Dhar. The draft of the manuscript is also prepared by the first author with the guidance of Dr. Ashutosh Dhar. The other authors mainly co-supervised the research and reviewed the manuscript.

4.1 Abstract

Buried pipelines, used for transporting oil, gas, and water, are often required to cross active landslide areas, which might be subjected to loads due to ground movements. The effects of the ground movement loads on the performance of buried pipelines is an important consideration for pipeline integrity assessment. Experimental and analytical studies have been conducted in the past for estimation of the maximum loads on pipelines due to ground movement. However, the existing approaches for the assessment of load on pipes subjected to ground movements are not well developed. This chapter presents a new laboratory test facility for pullout testing of buried pipelines, which is used to conduct tests of 178-mm diameter ductile iron pipes buried in sand. During the tests, the horizontal and vertical earth pressure in the soil was measured using Tekscan pressure sensors. A finite element (FE) modelling technique is also developed to investigate pullout behaviour. The

peak axial force obtained from laboratory tests for the pipe in dense and loose sands suggests that the current guidelines for predicting the maximum pullout force may not be applicable for ductile iron pipes in dense condition. The FE results show that the constrained dilation of sand near the pipe–soil interface and arching effects due to the greater stiffness of ductile iron pipe influence the mobilized load on the pipe.

4.2 Introduction

The landslide is a common geohazard which affects the performance of buried pipelines. Most of the pipelines carrying hydrocarbons and water are buried and are sometimes subjected to relative ground movements. The ground movements could be in a longitudinal, transverse, or oblique direction of the pipe, which causes external forces on the pipe in the direction of the movement. The ground load on pipelines subjected to axial ground movement is investigated in this chapter.

For the pipelines subjected to axial ground movement, the current design guidelines (e.g., ALA 2001) recommend Eq. (4.1) for estimating the maximum axial force.

$$R_a = \gamma' \pi D H \frac{1 + K_0}{2} tan\delta \qquad [4.1]$$

where R_a is the maximum axial force per unit length; γ' is the effective unit weight of soil; H is the burial depth measured from the pipe springline; D is the external pipe diameter; δ is the pipe–soil interface friction angle, and K_0 is the at-rest lateral earth pressure coefficient. Eq. (4.1) represents the maximum resistance offered by the soil against axial movement of the pipe.

Physical model tests were conducted in previous studies to investigate the loads on pipelines subjected to ground movements (e.g., Paulin et al. 1998, Wijewickreme et al. 2009; Daiyan et al. 2011; Sheil et al. 2018). A number of these studies showed that the ALA 2001 (Eq. 4.1) is not successful in calculating the pullout forces obtained in laboratory experiments. The discrepancies are attributed to the incorrect estimation of the normal stress on the pipe surface (Weerasekara and Wijewickreme 2008), which is a major challenge not only in pipelines but also in pile foundations (Randolph et al. 1994). The change of stress and strain fields in the soil during loading, under a low-stress condition for the typical pipeline burial depth, compound the problem. Wijewickreme et al. (2009) measured interface stresses in a laboratory pullout test of a 457-mm steel pipe buried in dry sand and found that the normal stress on the pipe increases during the axial pullout. The increase of normal stress is attributed to the dilation of soil at the pipe–soil interface. Sheil et al. (2018) also measured normal stress higher than the overburden pressure at the crown of a steel pipe. They described the higher normal stress as the rigid inclusion effect. However, no method is currently available to account for the dilation or rigid inclusion, due to lack of understanding about the effects. Muntakim and Dhar (2018) conducted three-dimensional (3D) FE analyses to investigate the pullout mechanisms of a medium-density polyethylene pipe and showed that the normal stress on the pipe is affected by an arching effect associated with the difference of the stiffness of the pipe with respect to the stiffness of the surrounding soil. No study is currently available on the pullout effects on buried ductile iron pipes, which are commonly used in municipal water distribution systems.

The main objectives of the present study are: (1) to develop a full-scale laboratory test facility to investigate the pipe–soil interaction during axial pullout of various pipes; (2) to investigate experimentally the pullout responses of ductile iron pipes using the developed facility; and (3) to examine the soil failure mechanisms and pipe–soil interaction during axial pullout for ductile iron pipe using FE analysis.

4.3 Test facility

A new full-scale laboratory test facility has been developed as a part of this study at Memorial University of Newfoundland. The facility has dimensions of 4 m (length) × 2 m (width) × 1.5 m (height). The testing cell was built using 6-mm thick steel plates. The stiffness of the cell walls was increased by adding 75 mm × 75 mm × 5 mm and 150 mm × 75 mm × 5 mm structural angle sections in the vertical and horizontal directions. FE analyses were performed to investigate potential boundary effects on test results during the design stage of the test facility (Murugathasan et al. 2018). The schematic drawings of the test cell are shown in Figure 4.1.

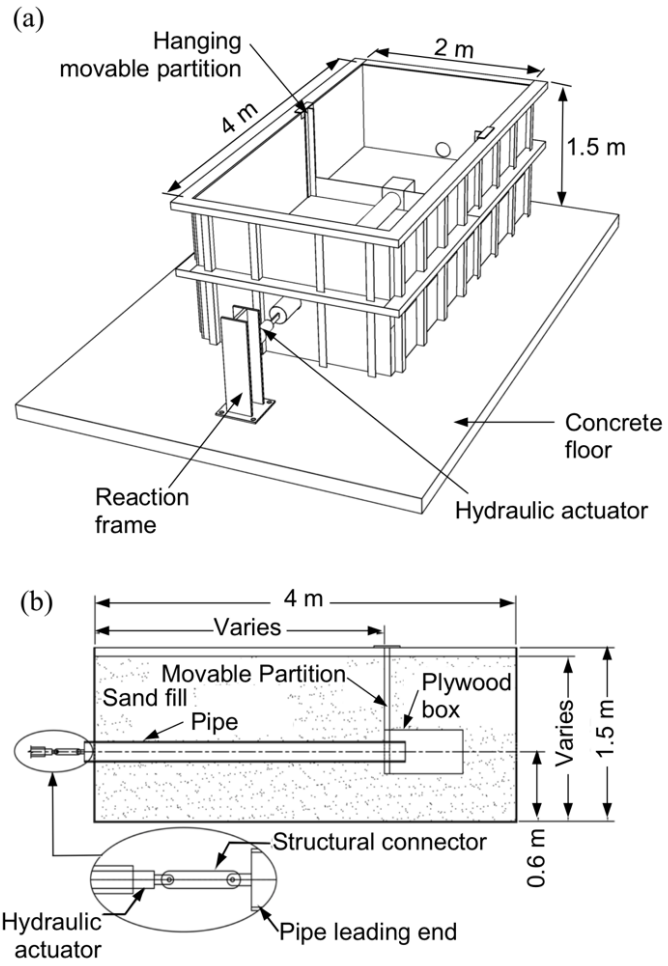

Figure 4.1. Schematics of the test facility: a) test cell, b) a longitudinal section

The test facility has two circular openings of adjustable sizes on two opposite walls in the long direction of the box that allow pullout testing of pipes with different diameters. A detachable partition system has been designed to facilitate testing of pipes of various lengths. The partition is built using a steel plate and angle bars that hold the pipe at the tailing end through an adjustable circular opening. A plywood box is used during the test to isolate the tailing end of the pipe from the sand when the tank is filled with sand. The arrangement of the partition system is shown in Figure 4.1(b). A structural connector

fabricated from a 12-mm thick steel plate is used to connect the pipe and actuator. The connection is shown in Figure 4.2. The openings in the tank walls and partition wall, through which the test pipe passes, are slightly larger than the outer diameter of the pipe. The gap is filled with lubricant (grease) to minimise the friction between the pipe and the face of the openings. A segment of a ductile iron water main having an external diameter (D) of 178 mm is tested in the facility to investigate the pullout behaviour. The side wall distance and bedding distance from the tests pipe are 5.5D and 3.3D, respectively (Figure 4.3). The pipe has a wall thickness of 12.7 mm.

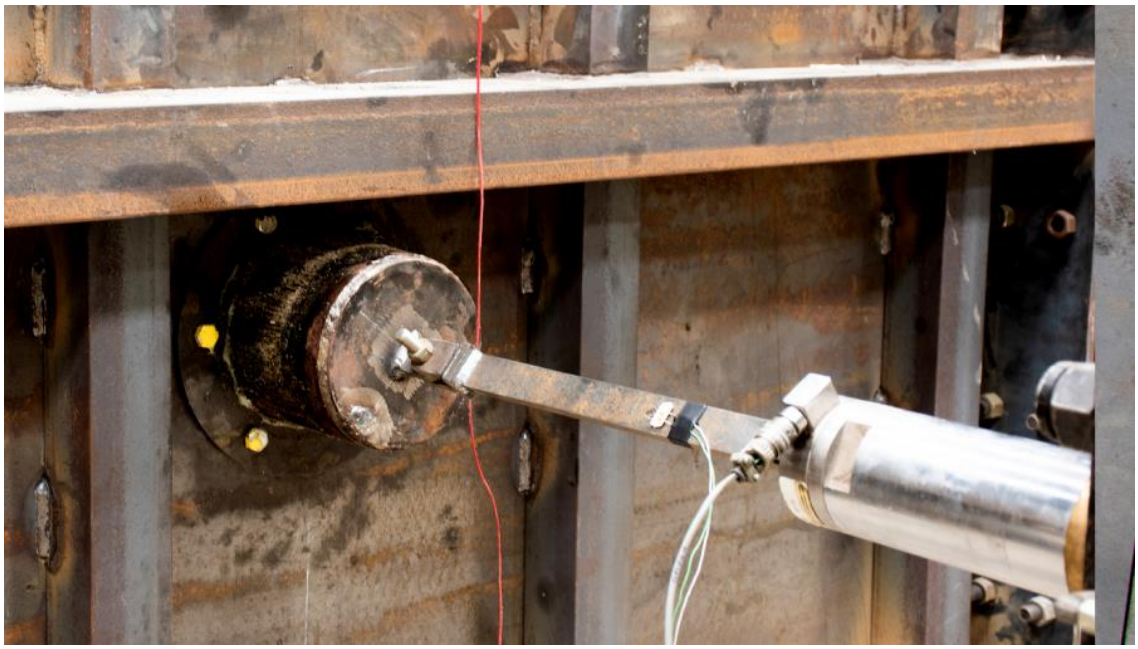

Figure 4.2. Connection details between the pipe and hydraulic actuator

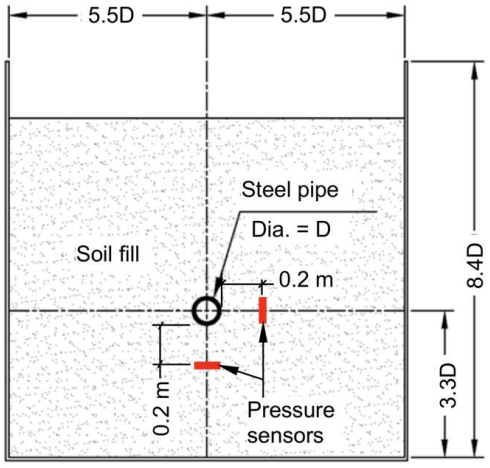

Figure. 4.3 Schematic view of test cell cross-section

4.4 Experimental program

4.4.1 Test materials and preparation

A locally available well-graded sand with the coefficient of uniformity C_u = 5.8 and coefficient of curvature C_c = 2.1 was used as the backfill material for the pipe. The sand was air dried with a moisture content of less than 1%. The minimum and maximum dry densities were 9.2 kN/m^3 and 19.3 kN/m^3, respectively. An overhead crane and bulk bags were used to move the soil in and out of the test cell. The sand was placed in layers having thicknesses of ~ 100 mm to 150 mm and then compacted manually to achieve the target soil density. The pipe was installed once the soil reached the targeted pipe bottom level (Figure 4.4). The soil was filled around the pipe up to the pipe springline level and compacted carefully to achieve the target density in that region. The soil backfilling was continued above the pipe springline up to the target cover depth, again in layers of 100-mm to 150-mm thickness. The final soil top surface was levelled using hand trowels. The soil density measurements were taken in different locations at various depths. All the tests were

conducted after 24 hours from the completion of filling, except for test T4. For test T4, the soil was filled without any compaction (as placed), and the test was conducted after an hour from completion of filling. A 2.7-m long segment of the pipe is tested.

Figure 4.4. Inner view of the test facility showing the pipe placement

4.4.2 Test cell instrumentation

Tekscan pressure sensors were used to monitor the earth pressures close to the pipe. The locations of the pressure sensors are shown in Figure 4.3. These pressure sensors were used to record the horizontal and vertical soil stresses at the pipe springline level by placing the sensors in the horizontal and vertical orientations, respectively. The vertical earth pressure

change below the pipe was also measured in a few tests. However, the main challenge involved with this type of Tekscan sensor was getting proper calibration for each use, because the area covered by the sensor was not consistent in each installation, due to different sand particle sizes and shapes. Strain gauges of 5-mm gauge length were used to measure the axial strain of the pipe and to measure the strain in the test cell's sidewalls to examine the rigidity of the cell wall.

4.4.3 Test program

A total of five pullout tests on ductile iron pipe segments was conducted (termed herein as Tests T1, T2, T3, T4 and T5). Each test was conducted by applying a displacement-controlled axial movement to the pipe. Test T1 was conducted at a pulling rate of 1 mm/sec while tests T2, T3 and T4 were performed at 0.5 mm/sec. A slower pulling rate of 0.017 mm/sec (1 mm/min) was used for test T5 to examine the influence of the pulling rate. In all five cases, the pipe was axially pulled to a displacement of 100 mm, except for T5, where the test was stopped when the load cell capacity was reached. The burial depth (H) in tests T1 and T2 was 690 mm (H/D = 3.87). In all other tests, the burial depth was 825 mm (H/D = 4.67). Tests T2, T3 and T5 were conducted in dense sand. Tests T1 and T4 were conducted in medium dense and loose sand, respectively. The sand was manually compacted to obtain the desired density (i.e., the relative density of about 75%–80%) for tests T2, T3 and T5, while no compaction was applied for test T4. Achieving the consistent target density was, however, very challenging, due to the difficulties in maintaining a constant compaction effort. Table 4.1 summarises the testing conditions encountered.

Table 4.1. Summary of pullout tests

Test No.	T1	T2	T3	T4	T5
Pulling rate, v (mm/s)	1.0	0.5	0.5	0.5	0.017
H/*D*	3.87	3.87	4.67	4.67	4.67
γ (kN/m^3)	15.7	17.03	17.17	15.11	17.76
Relative compaction (%)	80.4	88.2	88.4	77.9	91.6

4.4.4 Test results

Figure 4.5 shows the load–displacement curves obtained from the tests. The pullout force, which is essentially the same as the resistance offered by the surrounding soil, increases initially almost linearly with the pipe displacement and then becomes nonlinear. The linear load–displacement response is expected until the shear strength of the soil is mobilized during the pullout operation. After mobilization of the soil shear strength, the pullout force increases nonlinearly and reaches the peak value. The pullout resistance reduces slightly after the peak and the reduction continues until the end of the test.

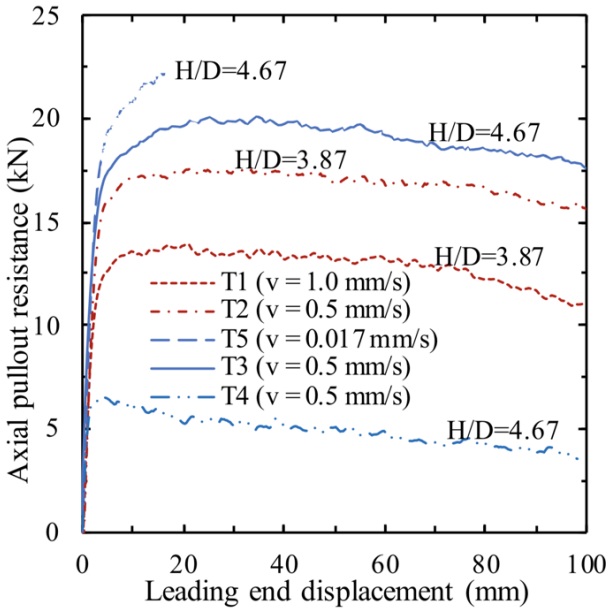

Figure 4.5. Pullout force versus leading end displacement for Tests T1–T5

As expected, the peak pullout resistance is higher in dense sand than in loose sand. For the pipes buried at the same depths (e.g., T3 and T5 or T1 and T2), a higher pullout force is obtained when the relative compaction of the soil is higher. The peak pullout force also depends on the burial depth. For the tests in soils having similar relative compaction (e.g., T2 and T3), the maximum pullout force is higher for the pipe having greater burial depth. Test T5 is conducted at a slow loading rate to examine the effect of loading. The maximum pullout force in this test is the highest. However, the relative compaction of the soil is also the highest for this test (Table 4.1). The high pullout force in Test T5 is likely due to the relatively high compaction of the backfill soil. The effect of loading rate on the shear strength of sand is expected to be insignificant (Saha et al. 2019).

The axial pullout force per unit length is normalised using Eq. (4.2) to facilitate the comparison of different test results. The normalized axial resistance (N_a)is defined as:

$$N_a = \frac{R_a}{\gamma \pi D H} \quad [4.2]$$

The normalized pullout resistances are plotted against pullout displacement in Figure 4.6. This shows that even though the maximum axial pullout resistance in test T3 is higher than the resistance in test T2, due to greater burial depth (Figure 4.5), the normalized pullout resistance is almost the same for these two tests. The relative compaction of the soil in these two tests is very similar. Thus, the maximum normalized pullout resistance is constant ($N_a \approx 1$) for the pipe if the backfill soil conditions are the same. Bilgin and Stewart (2009) revealed earlier that for cast iron pipes, the shearing resistance against the axial pullout depends only on the burial depth if the soil condition is the same. They proposed a simplified expression of the interface shearing resistance in terms of a constant and the burial depth, *H*. For dense sand, the unit interface shear resistance was expressed as 14.0*H* for the cast iron pipe. For the ductile iron pipe used in this study, the shearing resistance is ~ 16.0*H*–17.0*H*, which is slightly higher than the value recommended in Bilgin and Steward (2009) for cast iron pipe.

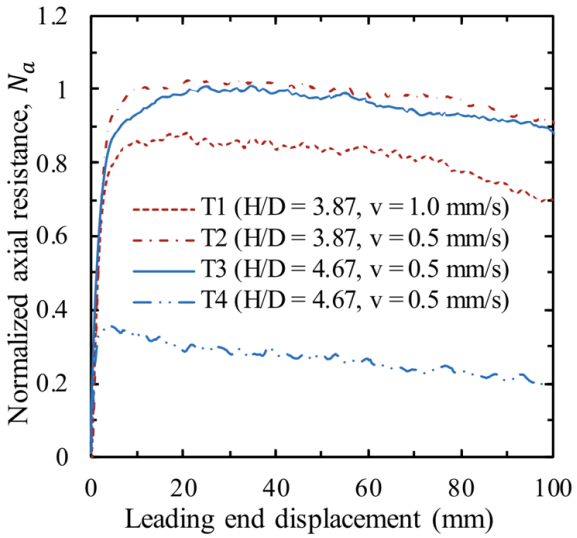

Figure 4.6. Normalized pullout resistances (Tests T1–T4)

The normalized pullout resistance also reduces with the reduction of the relative compaction of the sand. For medium dense sand (test T1) and loose sand (test T4), the maximum normalised pullout resistance is approximately 0.86 and 0.36, respectively. The unit interface shearing resistance for the ductile iron pipe is calculated to be 13.0*H* and 5.0*H*, compared to the shearing resistance of 9.3*H* and 6.0*H* for the cast iron pipe reported in Bilgin and Steward (2009). In general, the maximum pullout force in dense sand is 1.3 times and 3.2 times the pullout force in medium dense and loose sands, respectively.

The soil stresses measured during the pipe pullout are shown in Figure 4.7. The stresses in the immediate vicinity of the pipe could not be measured using the Tekscan sensor due to the positioning difficulties. Therefore, the soil stresses at 200 mm below the invert of pipe and 200 mm away from the pipe surface at the springline level were measured. No significant changes occurred in the vertical stress below invert and the horizontal stress at

the springline level for both loose and dense conditions of the sand. This implies that the shearing zone around pipe–soil interface did not influence the stress field at a distance of 200 mm from the pipe surface during the axial pullout.

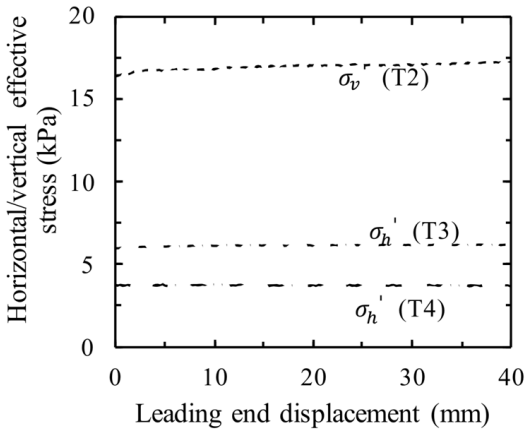

Figure. 4.7. Variation of soil stresses during axial pullout

The pipe axial strain is measured at mid-length in one of the tests (test T1). The results are shown in Figure 4.8. The strain remains constant initially and increases during the pullout until the peak resistance is mobilized. The strain magnitudes are in a negligible order (10^{-5}), indicating that the pipe moves as a rigid body during axial pullout.

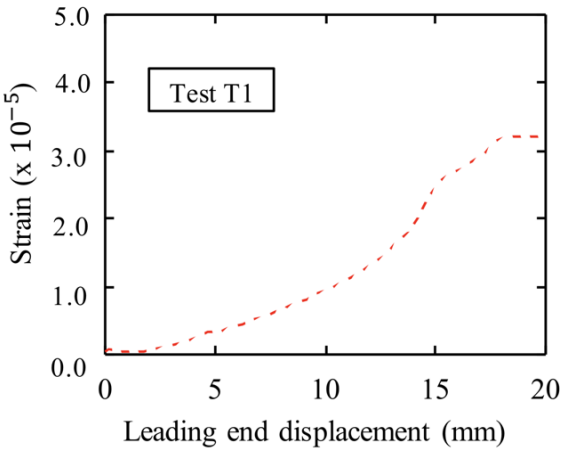

Figure 4.8 Pipe wall strain during axial pullout

The strain gauges which are attached to the test cell side walls, are monitored during the pullout tests. Figure 4.9 shows the strain gauge readings with time during tests T3 and T4. The readings were recorded before and during the pulling process. Pulling was initiated at 20 sec for both tests and the maximum resistance was reached at 60 sec and 45 sec for tests T3 and T4, respectively. It is noted that there is no indication of an increase in wall strain during the pulling of the pipes both in dense and loose sands. Thus, the boundary walls do not have any influence on the pipe–soil interaction during axial pullout.

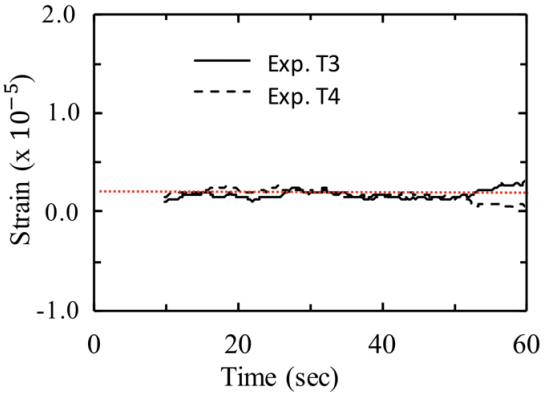

Figure 4.9. Strain gauge readings on the side wall of the test cell during axial pullout

4.5 Numerical modelling of axial pullout

4.5.1 Finite element modelling

Numerical modelling of the axial pullout is conducted using the commercially available Abaqus/Standard FE software (Dassault System, 2014). Three-dimensional (3D) analyses are performed, since 2-D modelling is not suitable for modelling the axial pullout response of pipe. The pipe tests with dense and loose backfill soil having the same burial depth (tests T3 and T4) are analysed to investigate the mechanisms during axial pullout in these soil conditions. Taking advantage of the symmetry of the problem, only one half of the problem is modelled to make the analysis computationally efficient. The soil and the pipe are modelled as deformable bodies using eight node linear brick elements (C3D8R). The FE mesh used in the model is shown in Figure 4.10. A finer mesh is used in the close vicinity of the pipe while a coarser mesh is used away from the pipe. The pipe is extended beyond the test cell boundary at the front and rear ends so that the total length of contact of the soil with the pipe remains unchanged during axial pullout (similar to the laboratory tests).

The strains measurement during the laboratory tests indicated that there are no significant changes in the wall strain of the test cell during the pipe pullout (Figure 4.9). Therefore, it is considered reasonable to idealize the boundary walls as rigid. Thus, the horizontal translational degrees of freedom are restricted for the vertical faces of the boundaries. For the bottom boundary, both horizontal and vertical degrees of freedom are restrained. Symmetrical boundary conditions are applied to the pipe and soil on the symmetrical plane.

In the numerical model, the self-weight of soil and pipe are first applied in the gravity step to generate the initial stresses in the domain. The generated horizontal soil stresses are examined and are found to be very close to the lateral earth pressures at K_0 condition (i.e., $(\nu/(1-\nu)\,)\sigma_v')$. In the subsequent step, the axial pullout is simulated by applying a velocity boundary condition on the pipe nodes at the leading end.

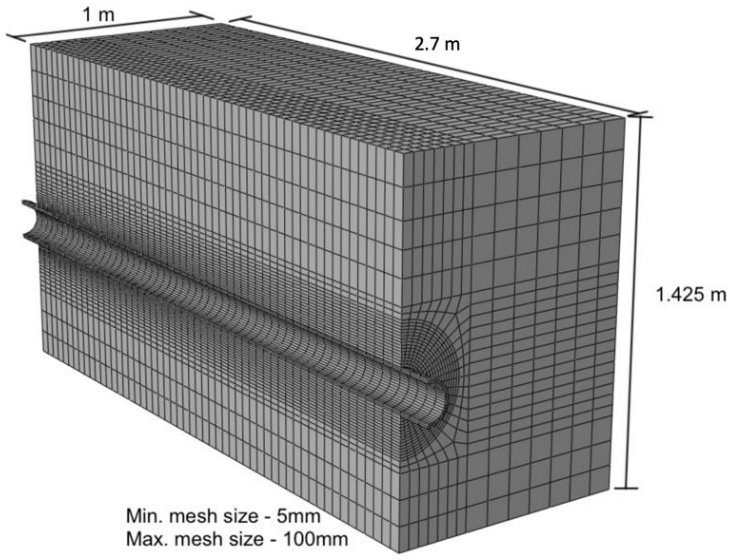

Figure. 4.10 Typical FE mesh used in finite element analysis

4.5.2 Soil parameters and material models

The built-in elastic-perfectly plastic model with Mohr-Coulomb (MC) plasticity, available in Abaqus, is employed to model the stress–strain behaviour of the sand. The soil is assumed to behave elastically until the stress state reaches the MC failure criteria (yield surface). Once the soil stress state reaches the failure (yield) surface, plastic strains develop in the soil and the soil dilates at a constant dilation angle. Although the soil in the field may experience plastic strains before it reaches the MC criteria and may have a non-constant

dilation angle, the conventional MC model could be successfully used to estimate the ultimate soil resistance during the axial pullout (Muntakim and Dhar 2018). Yimsiri et al. (2004) also showed that the conventional MC model can provide a reasonable response in a pipe-soil interaction simulation. The parameters required for this model are Young's Modulus (E), Poisson's ratio (ν), angle of internal friction (ϕ'), and dilation angle (ψ_m). Furthermore, the unit weight of the soil (γ) is required to simulate the gravity load.

In the current analysis, a peak friction angle of 38° and the critical state friction angle of 33° are considered to model the dense sand behaviour (after Saha et al. 2019). A dilation angle of 8° is estimated using Eq. (4.3) (Bolton 1986), which defines the maximum dilation angle (ψ_m) in terms of peak friction angle (ϕ'_{peak}) and critical state friction angle (ϕ'_{cv}). To simulate the loose sand condition, the friction angle of 30° is used along with a minimum (0.1°) dilation angle (Saha et al. 2019). A small cohesion of 0.1 kPa and a minimum dilation angle for loose sand are applied for numerical stability during analysis.

$$\psi_m = \frac{\phi'_{\text{peak}} - \phi'_{\text{cv}}}{0.8} \quad [4.3]$$

The Young's modulus of soil is estimated using Eq. (4.4) (Hardin and Black 1966; Janbu 1963).

$$E = Kp_a\left(\frac{p'}{p_a}\right)^n \quad [4.4]$$

where K is a material constant; p_a is the atmospheric pressure (100 kPa); p' is mean effective confining pressure; and n is an exponent. This power function is widely used in the

numerical modelling of pipe–soil interaction problems (Yimsiri et al. 2004; Guo and Stolle 2005; Daiyan et al. 2011; Jung et al. 2013). The value of E is estimated based on the mean effective stress (p') at the springline level of the pipe with K = 150 and n = 0.5 (Roy et al. 2015) as E = 5 MPa for dense sand and E = 3 MPa for loose sand. A constant Poisson's ratio of 0.3 is assumed for both loose and dense sand.

Table 4.2 Parameters used in FE analyses (modelling of axial pullout)

Parameter	Dense sand	Loose sand
E (MPa)	5	3
ν	0.3	0.3
ϕ'(°)	38	30
ψ_m (°)	8	0.1
Density of soil, ρ(kg/m^3)	1750	1540
Cohesion[a], c' (kN/m^2)	0.1	0.1
Interface friction coefficient, μ	0.74	0.43
Depth of pipe, H/D	4.67	4.67

[a]a small value of cohesion is used in the Mohr–Coulomb model in Abaqus for numerical stability

The surface to surface contact approach available in Abaqus is used to simulate the contact between the pipe and the soil. With this method, the sliding occurs when the shear stress at the contact interface reaches the critical shear stress. The critical shear stress is simply the friction coefficient (μ = tanδ) times the normal stress. The value of δ depends

on the interface roughness between the two mediums. In general, the value of δ falls in the range of 50% to 100% of the peak angle of internal friction of the surrounding soil. ALA (2001) recommends the value of μ be between 0.6 and 1.0, depending on the type of surface coating of pipe. The pipe–soil interface friction coefficients of 0.74 and 0.43 are used for dense and loose sand, respectively, which simulate successfully the test conditions. The corrosion coating on the pipe might have contributed to the higher value of wall friction. These friction values correspond to an angle of wall friction of 95% of the angle of internal friction of the soil ($\delta = 0.95\phi$) for both dense and loose sand. The parameters used in the FE models are summarized in Table 4.2. The modulus of elasticity and Poisson's ratio of pipe material are assumed to be 200 GPa and 0.3, respectively.

4.5.3 Comparison of results

Figures 4.11 and 4.12 compare the pullout resistances from the FE analyses with those from the laboratory tests for pipes buried in dense and loose sand, respectively. The results of FE analyses are in reasonable agreement with the full-scale test results in the figures where the peak pullout forces are effectively calculated by the FE method. As expected, the post-peak response was not successfully simulated by the present FE analyses performed because of using the conventional MC model (constant friction dilation angle) for the soil.

The normalized axial resistances obtained from the laboratory tests are also compared with those obtained using ALA (2001) guidelines (Figures 4.11 & 4.12). In ALA (2001), the at-rest lateral earth pressure coefficient (K_0) value is used to calculate the peak

resistance. However, in the comparison in Figures 4.11 and 4.12, a lateral earth pressure coefficient value (K_1) is back-calculated using ALA (2001) equation to match the experimental results. The back-calculated value of K_1 is 0.42 for loose sand, which is close to the value given by Jaky's Equation (i.e., 1-sinϕ'). For dense sand, the value K_1 is back-calculated to be 1.6. Thus, ALA (2001) equation with K_0 from Jaky's equation can be used to calculate the maximum pullout force for ductile iron pipe in loose sand while the equation with a higher value for the coefficient of lateral earth pressure provides the maximum pullout force for dense sand. Similar conclusions were drawn for steel pipes by Wijewickreme et al. (2009) where ALA (2001) equation was found to be applicable for loose soil and K_1 = 2.6 was found to calculate the maximum pullout force in dense soil.

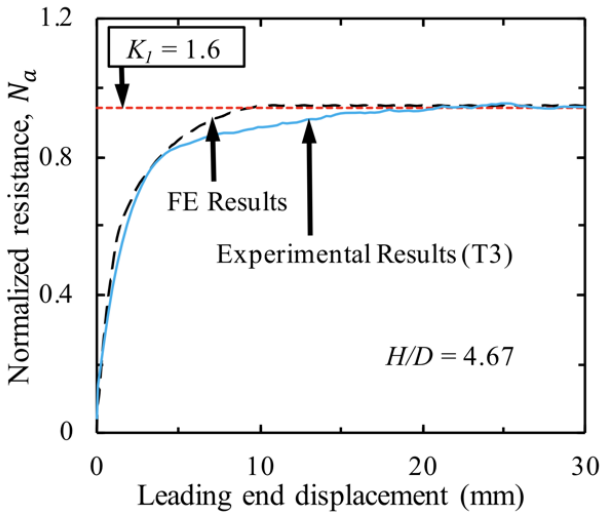

Figure 4.11 Comparison of full-scale test and finite element load–displacement responses in dense sand

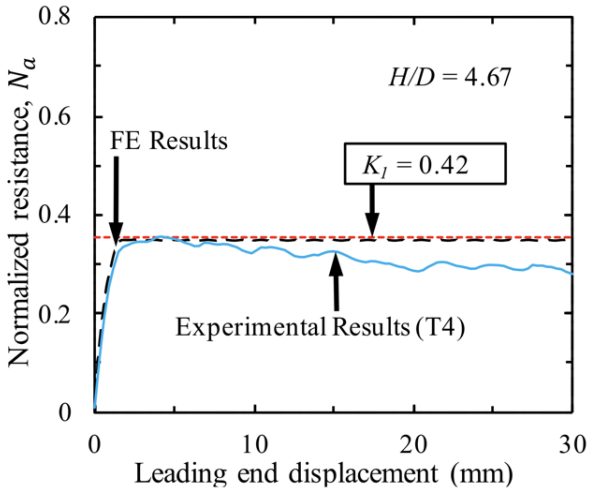

Figure 4.12 Comparison of full-scale test and finite element load–displacement responses in loose sand

4.6 Mechanism of soil-pipe interaction

The laboratory investigation presented here as well as those published in the literature reveal that the current design guidelines (ALA 2001) cannot always be applied in calculating the pullout resistance of buried pipelines. Previous studies proposed using a different coefficient of lateral earth pressure (Wijewickreme et al. 2009 & Sheil et al 2018) to ALA (2001) equation to match their experimental results. Although the experimental studies provide valuable data on the global response of the pipes, the mechanisms of pipe–soil interaction cannot be properly measured during the tests. However, the mechanism of soil–pipe interaction during axial pullout must be properly understood for developing an improved design method for the buried pipelines. Wijewickreme et al. (2009) postulated that constrained soil dilation occurs at the interface during axial pulling of pipes buried in dense sand, which causes higher normal stress than the one given by the design equation.

To simulate the effects of interface soil dilation using two-dimensional numerical analysis, they applied a radial expansion of the pipe by an amount of an estimated dilation. In the current study, 3D FE analysis is employed to investigate the mechanism of soil–pipe interaction including the soil dilation during axial pullout of ductile iron pipe. As discussed above, the FE analysis is found to simulate successfully the test conditions.

Since the mobilization of shearing resistance is expected to depend on the relative movement of the pipe with respect to the surrounding soil, the axial strain at different points along the length of the pipe is examined in Figure 4.13. The figure includes axial strains at the distances of one-quarter, one-half and three-quarters of pipe length ($L/4$, $L/2$ and $3L/4$) from the leading end, along with pipe length elongation. As observed in the measurement (Figure 4.8), the order of magnitude of the strains are very much less in Figure 4.13. For both loose and dense sand, higher axial strains are observed at the distance of one-quarter, which reduced subsequently along the pipe length. However, since the axial strain is very small, the pipe can be considered to move as a rigid body (calculated elongation is 0.007 mm to 0.02 mm).

The average normal stresses (normal stress averaged over the pipe circumference) are also examined at the three distances, as shown in Figure 4.14. For loose sand, the average normal stresses at three locations are very close to each other and remain constant during the axial pullout. There is no effect of soil dilation, as a small value of the angle of dilation is used. However, for the pipe in dense sand, normal stresses increase from the initial values and reach the maximum value at the leading end displacement corresponding to the peak pullout force. The increase of normal stress is associated with the use of a dilation angle of

8°. Note that the effect of dilation (normal stress increase) is higher toward the tailing end of the pipe.

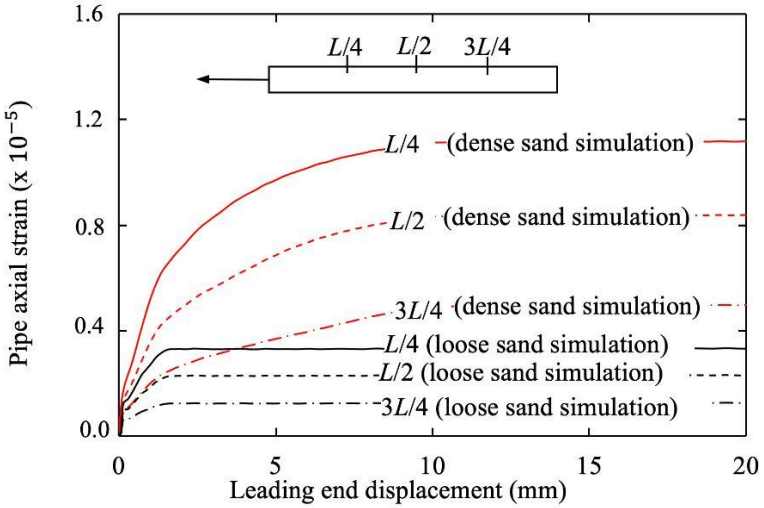

Figure 4.13 Axial strain along pipe length from FE analysis

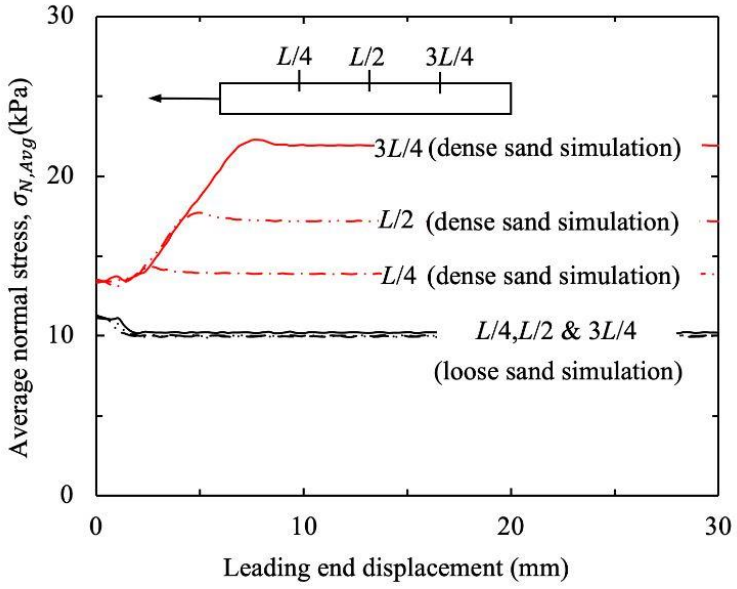

Figure 4.14 Normal stress along pipe length from FE analysis

Figure 4.15 shows the circumferential distribution of average normal stresses normalized by the effective overburden pressure at the relevant depth, corresponding to the maximum pullout force. In both dense and loose sand conditions, normalized normal stresses at the pipe crown and pipe invert levels after the gravity load step are greater than 1, indicating that the normal stress is greater than the effective overburden pressures. Higher stresses at the crown and invert are caused by negative arching, due to the greater stiffness of pipe than the stiffness of the surrounding soil. The stress at the invert is also contributed to by the self-weight of the pipe. The normal stress at the pipe springline level is found to be very close to the effective horizontal soil stress at that level. The normal stresses around the pipe increase during the axial pullout for the pipe in dense sand while no significant change is noted for loose sand. As discussed earlier, for the simulation of the pipe response in dense sand, a constant dilation angle of 8° is applied, while no dilation (a minimum value) is considered for the simulation of the pipe in loose sand. The increase in the normal stresses in the FE calculation for dense sand is thus due to the use of the angle of dilation. The results of analyses confirm that the normal stress increases during axial pullout due to soil dilation, resulting in a higher pullout resistance for pipes in dense sand. The FE analysis with a constant dilation angle could successfully simulate the maximum pullout resistance.

Dilation of soil occurs due to plastic deformation of the soil. The plastic shear strains (plastic strain magnitude PEMAG in Abaqus) around the pipe circumference are plotted in Figure 4.16, when the pullout force reaches the maximum value. This shows that plastic strains are developed within a thin zone of soil around the pipe.

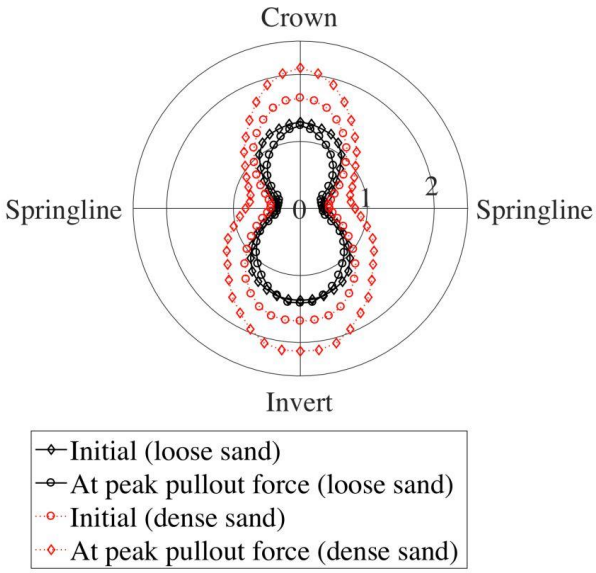

Figure 4.15 Distribution of normal stresses around the pipe circumference

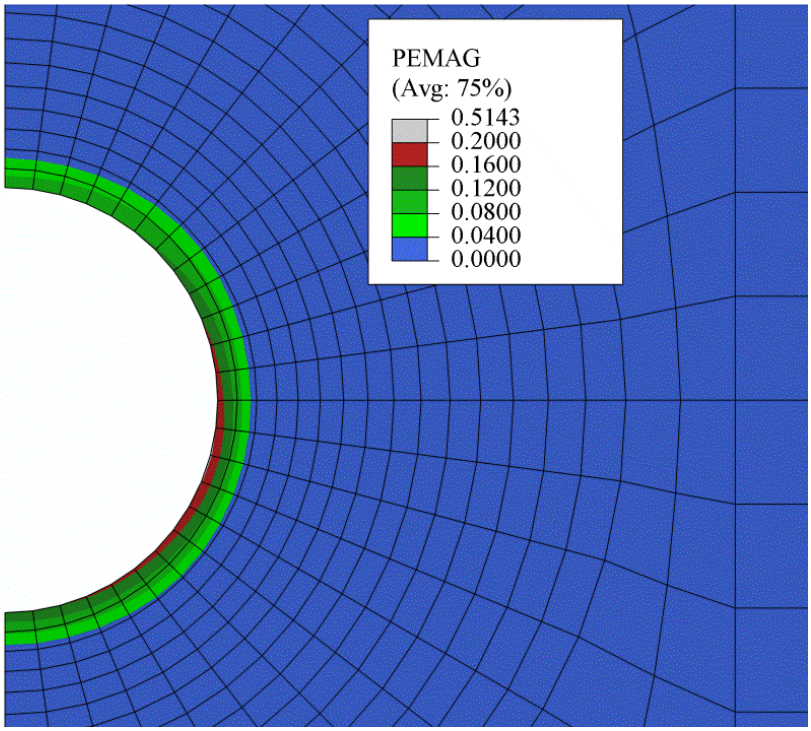

Figure 4.16 Plastic deformation of soil around the pipe

4.7 Conclusions

A new test facility developed for axial pullout testing of ductile iron pipe is presented in this chapter. Five axial-pullout tests of a ductile iron pipe (water main) are conducted using the facility to examine the pullout resistance under various conditions, including different pipe burial depths, relative densities of soil, and pulling rates. Three-dimensional finite element analysis is conducted to analyse the test results and investigate the mechanisms of soil-pipe interaction during axial pullout of the pipes. The major findings from the research are listed below.

- Axial pullout force is significantly affected by the relative density of the soil. The maximum pullout force in dense sand is found to be 1.3 times and 3.2 times the pullout force in medium dense and loose sand, respectively.
- For pipes in soil having similar relative compaction, the maximum pullout force is greater for the pipe with increased burial depth. However, the pullout force normalized by the burial depth is constant. Thus, a simplified method of calculating the unit interface shearing resistance as a constant times the burial depth (H) can be used for ductile iron pipe. The unit interface shear resistance is found to be 16.0H to 17.0H in dense sand, 13.0H in medium dense sand and 5.0H in loose sand for the pipes tested.
- The maximum pullout resistances are successfully calculated with ALA (2001) equation using the coefficient of lateral earth pressure, K_1 of 0.42 for loose sand and 1.6 for dense sand. The value K_1 for loose sand is close to the value given by Jaky's equation. Thus, ALA (2001) equation with K_0 from Jaky's equation

can be used to calculate the maximum pullout force for ductile iron pipe in loose sand, while the equation with a higher value for the coefficient of lateral earth pressure provides the maximum pullout force for the pipe in dense sand.

- Three-dimensional FE analysis with the conventional Mohr–Coulomb plasticity model using a constant friction and dilation angles could successfully simulate the soil–pipe interaction of ductile iron pipe. The results of FE analysis confirm that the increase of pullout resistance in dense sand is due to dilation of the soil, which increases the normal stress on the pipe. The dilation of soil occurs within a thin zone around the pipe. Analysis with a negligible dilation angle successfully simulates the pullout behaviour of a pipe in loose sand.
- Arching due to higher stiffness of the ductile iron pipe with respect to the surrounding soil contributes to normal stress on the pipe.

Acknowledgments

The authors gratefully acknowledge the financial support for this research provided by the National Science and Engineering Research Council of Canada. Financial support is also provided from the SBM grants of Memorial University of Newfoundland, Mitacs and PRNL.

References

American Lifelines Alliance. 2001. Guidelines for the design of buried steel pipe. American Lifelines Alliance in partnership with the Federal Emergency Management Agency and American Society of Civil Engineers, Washington, D.C. Available from www. americanlifelinesalliance.org [accessed 13 April 2019].

Bilgin, Ö. and Stewart, H. E., 2009. Pullout resistance characteristics of cast iron pipe. Journal of Transportation Engineering, **135**(10): 730–735.

Bolton, M.D. 1986. The strength and dilatancy of sands. Géotechnique, **36**(1): 65–78. doi:10.1680/geot.1986.36.1.65.

Daiyan, N., Kenny, S., Phillips, R., and Popescu, R. 2011. Investigating pipeline-soil interaction under axial–lateral relative movements in sand. Canadian Geotechnical Journal, **48**(11): 1683–1695. doi:10.1139/t11-061.

Guo, P., and Stolle, D. 2005. Lateral pipe-soil interaction in sand with reference to scale effect. Journal of Geotechnical and Geoenvironmental Engineering, **131**(3):338−349.

Hardin, B.O., and Black, W.L. 1966. Sand stiffness under various triaxial stress. Journal of the Soil Mechanics and Foundations Division, ASCE, **92**(SM2): 27– 42.

Janbu, N. 1963. Soil compressibility as determined by oedometer and triaxial tests. In Proceedings, European Conference on Soil Mechanics and Founda- tions Engineering, Wiesbaden, Germany. Vol. 1, pp. 19–25.

Jung, J., O'Rourke, T., and Olson, N. 2013. Lateral soil-pipe interaction in dry and partially saturated sand. Journal of Geotechnical and Geoenvironmental Engineering, **139**(12): 2028−2036.

Muntakim, A.H., and Dhar, A.S. 2018. Investigation of axial pullout behaviour of buried polyethylene pipelines. Newsletter, International Association for computer methods and advances in Geomechanics, Vol. 23.

Murugathasan, P., Dhar, A. and Hawlader, B. 2018. A laboratory facility for studying pullout behaviour of buried pipelines. Annual conference of Canadian Geotechnical Society, GeoEdmonton2018, AB, Canada.

Paulin, M. J., Phillips, R., Clark, J. I., Trigg, A., and Konuk, I.1998. A full-scale investigation into pipeline/soil interaction, International pipeline conference '98, ASME, Calgary, Alberta, Canada, 2: 779–788.

Randolph, M.F., Dolwin, R., and Beck, R. 1994. Design of driven piles in sand. Géotechnique, **44**(3): 427–448. doi.org/10.1680/geot.1994.44.3.427.

Roy, K., Hawlader, B., Kenny, S. and Moore, I., 2015. Finite element modeling of lateral pipeline–soil interactions in dense sand. Canadian Geotechnical Journal, **53**(3): 490–504. doi.org/10.1139/cgj-2015-0171.

Saha, R. C., Dhar, A., Hawlader, B. 2019. Shear strength assessment of a well-graded clean sand. Annual conference of Canadian Geotechnical Society, GeoSt.John's 2019, St.John's, NL, Canada.

Sheil, B. B., Martin, C. M., Byrne, B.W., Plant, M., Williams, K., and Coyne, D. 2018. Full-scale laboratory testing of a buried pipeline in sand subjected to cyclic axial displacements. Géotechnique, **68**(8): 684–698. doi.org/10.1680/jgeot.16.P.275.

Weerasekara, L., and Wijewickreme, D. 2008. Mobilization of soil loads on buried, polyethylene natural gas pipelines subject to relative axial displacements. Canadian Geotechnical Journal, **45**(9): 1237–1249. doi:10.1139/T08-043.

Wijewickreme, D., Karimian, H., and Honegger, D. 2009. Response of buried steel pipelines subjected to relative axial soil movement. Canadian Geotechnical Journal, **46**(7): 735–752. doi:10.1139/T09-019.

Yimsiri, S., Soga, K., Yoshizaki, K., Dasari, G., and O'Rourke, T. 2004. Lateral and upward soil-pipeline interactions in sand for deep embedment conditions. Journal of Geotechnical and Geo- environmental Engineering, **130**(8):830–842. doi:10.1061/(ASCE)10900241(2004)130:8(830).

Notations

ALA	American Lifeline Alliance
2D	two dimensional
3D	three dimensional
FE	Finite Element
MC	Mohr-Coulomb
C_c	coefficient of curvature
C_u	coefficient of uniformity
D	external diameter of the pipe
E	Young's modulus
H	distance of pipe centre from soil surface
K	material constant
K_1	lateral earth pressure coefficient
K_0	at-rest lateral earth pressure coefficient
L	length of pipe
n	power exponent
N_a	normalized axial pullout resistance
p'	mean effective stress

p_a atmospheric pressure (100kPa)

R_a maximum axial resistance per unit length

δ interface friction angle

γ unit weight of soil

γ' effective unit weight of soil

μ friction coefficient

ν Poisson's ratio

ϕ' angle of internal friction of soil

ϕ'_{cv} critical state friction angle

ϕ'_{peak} peak friction angle

ψ_m maximum dilation angle

σ'_v vertical effective stress

σ'_h horizontal effective stress

$\sigma_{N,Avg}$ average normal stress

CHAPTER 5

Summary and Recommendations for Future Work

5.1 Overview

The pipeline integrity assessment under axial ground loads is an important design consideration in order to build a safe and reliable water transportation pipeline network. Full-scale laboratory tests are an effective approach to study the pipe–soil behavior under axial loads. This thesis focuses on the design of a laboratory facility for axial pullout testing of buried pipelines and investigation of buried ductile iron pipelines subjected to axial pullout loads. In this chapter, a brief summary and a few general conclusions drawn from this thesis are discussed. The specific conclusions related to each problem are discussed in Chapters 3 and 4.

5.2 Conclusions

The following presents the key findings about the design of test cell for pullout testing of pipe and the results of experimental and numerical study on the behavior of ductile iron pipe subjected to axial pullout.

- The lateral deformation of the cell walls should be minimized to mimic the in-situ soil stress condition in the test cell. The lateral deformation of cell wall could be efficiently controlled by designing the cell wall with adequate stiffeners.

- The distance between side wall of cell and pipe should be sufficient enough to ensure that physical boundary does not affect the pipe-soil interaction behavior.

This study suggests that he side wall distance of 1 m (10D) is sufficient to minimize the boundary effects; however, it depends on the amount of dilation that occurs in the pipe-soil interface.

- The cell-soil interface friction angle could have moderate effects on the pipe-soil interaction unless it is minimized. The use of lubricated polyethylene sheets in the inner face of cell wall is one of the effective methods to reduce the friction between the cell wall and soil. However, the effect of cell-soil interface friction is found to be insignificant for the current purpose of tests.

- Relative density of the soil significantly effects the axial pullout force. The maximum pullout force in dense sand is found to be 1.3 times the pullout force in medium dense sand and 3.2 times the pullout force in loose sand.

- The pipe with a higher cover depth shows a greater maximum pullout force where the relative compaction is similar. However, the pullout force normalized by the cover depth remains constant. Thus, a simplified method (a constant times cover depth) is proposed to calculate the unit interface shearing resistance for ductile iron pipe. The unit interface shear resistance for dense sand, medium dense sand and loose sand is found to be 16.0H to 17.0H, 13.0H, and 5.0H, respectively.

- The ALA (2001) equation is used to back calculate the lateral earth coefficient (K_1) for loose sand and dense sand as 0.42 and 1.6, respectively. The calculated K_1 value of loose sand is close to the K_0 value calculated from Jacky's equation. Thus, the equation suggested in ALA (2001) along with K_0 from Jack's equation could be

successfully used to calculate the maximum pullout force for the pipes in loose sand. However, for the pipes buried in dense sand, a higher lateral earth pressure coefficient (>1) should be employed to acheive the maximum pullout force.

- The simple Mohr–Coulomb plasticity model which is defined using a constant friction and dilation angles, could be successfully used in the three-dimensional finite element modelling to study the axial pullout behavior ductile iron pipe. The FE analysis results affirm that normal stress increase on the pipe due to the dilation of soil contributes to the higher pullout resistance in dense sand. The dilation of soil occurs within a thin zone around the pipe. A minimum value of dilation angle used in the analysis shows the rational behavior of pipe in loose sand.

- The FE model response identifies that the arching effect which arises due to higher stiffness of ductile iron pipe relative to the encompassing soil also contributes to the increase in normal stress on the pipe.

5.3 Recommendations for Future Study

The following presents recommendations for future works related to this study.

- The present study considers different burial depths, pulling rates and relative compactions. In addition, the effect of various pipe lengths and pipe thicknesses can be considered in the future for a deeper investigation of the arching effect.
- The pipe pullout was only considered in one direction in the current sets of tests; however, reversing the pullout direction and applying the pullout several times in the same fill condition can be considered to assess the effect of cyclic loading.
- Lateral loading test of ductile iron pipe can be considered to investigate the lateral pipe-soil interaction behavior.
- The present numerical analysis identified that the axial pipe strain is not uniform along the pipe length. In the current tests, pipe strain was measured only in the middle of the pipe. Measuring the pipe strain at various points along the pipe length can be considered to identify the effects arises due to pipe elongation.
- A parametric study using the current numerical model can be undertaken to investigate the effects of different soil parameters on the pipe-soil response.
- In the current finite element model, the Mohr-Coulomb material model was employed to model the soil plasticity. A more advanced soil constitutive model can be used in the future to rationally idealize soil behavior.

REFERENCES (General)

Abaqus. (2016). Abaqus user's guide. Dassault Systèmes. Available from http://130.149.89.49:2080/v2016/books/usb/default.htm

Alam, S. and Alloche, E.N. 2010. Experimental investigation of pipe soil friction coefficients for direct buried PVC pipes, Pipeline Division Specialty Conference 2010, ASCE, Keystone, Colorado, USA, 2: 1160–1169.

Almahakeri, M., Moore, I., and Fam, A. 2016. Numerical study of longitudinal bending in buried GFRP pipes subjected to lateral earth movements, Journal of Pipeline Systems Engineering and Practice, **8**(1): 702–710.

American Lifelines Alliance. 2001. Guidelines for the design of buried steel pipe. American Lifelines Alliance in partnership with the Federal Emergency Management Agency and American Society of Civil Engineers, Washington, D.C. Available from www. americanlifelinesalliance.org [accessed 13 April 2019].

AWWA C-151. 2009. American national standards for Ductile-Iron pipe, centrifugally cast, for water. American Water Works Association. Available from http://dx.doi.org/10.12999/AWWA.C151.09.

American Water Works Association. 2011. "Buried No Longer: Confronting America's Water Infrastructure Challenge." American Water Works Association. Available from http://www.allianceforwaterefficiency.org/uploadedFiles/Resource_Center/Landing_Pages/AWWA-BuriedNoLonger-2012.pdf

Bilgin, Ö. and Stewart, H. E., 2009. Pullout resistance characteristics of cast iron pipe. Journal of Transportation Engineering, **135**(10): 730–735.

Bolton, M.D. 1986. The strength and dilatancy of sands. Géotechnique, **36**(1): 65–78. doi:10.1680/geot.1986.36.1.65.

Brachman, R.W., Moore, I.D., and Rowe, R.K. 2000. The design of a laboratory facility for evaluating the structural response of small-diameter buried pipes, Canadian Geotechnical Journal, **37**(2):281–295.

Daiyan, N., Kenny, S., Phillips, R., and Popescu, R. 2011. Investigating pipeline-soil interaction under axial–lateral relative movements in sand. Canadian Geotechnical Journal, **48**(11): 1683–1695. doi:10.1139/t11-061.

Dickin, E. 1994. Uplift resistance of buried pipelines in sand. Soils and Foundations, **34**(2): 41–48.

Folkman, S. 2018. Water Main Break Rates In the USA and Canada: A Comprehensive Study. Mechanical and Aerospace Engineering Faculty Publications. Paper 174. Available from https://digitalcommons.usu.edu/mae_facpub/174.

Guo, P., and Stolle, D. 2005. Lateral pipe-soil interaction in sand with reference to scale effect. Journal of Geotechnical and Geoenvironmental Engineering, **131**(3):338−349.

Ha, D., Abdoun, T.H., O'Rourke, M.J., Symans, M.D., O'Rourke, T.D., Palmer, M.C. and Stewart, H.E. 2008. Buried high-density polyethylene pipelines subjected to normal and

strike-slip faulting — a centrifuge investigation, Canadian Geotechnical Journal, **45**(12): 1733–1742.

Hardin, B.O., and Black, W.L. 1966. Sand stiffness under various triaxial stress. Journal of the Soil Mechanics and Foundations Division, ASCE, **92**(SM2): 27– 42.

Janbu, N. 1963. Soil compressibility as determined by oedometer and triaxial tests. In Proceedings, European Conference on Soil Mechanics and Founda- tions Engineering, Wiesbaden, Germany. Vol. 1, pp. 19–25.

Jung, J., O'Rourke, T., and Olson, N. 2013. Lateral soil-pipe interaction in dry and partially saturated sand. Journal of Geotechnical and Geoenvironmental Engineering, **139**(12): 2028−2036.

Karimian, H. 2006. Response of buried steel pipelines subjected to longitudinal and transverse ground movement, Ph.D. thesis, Department of Civil Engineering, The University of British Columbia, Vancouver, B.C.

Kroon, David H.; Linemuth, Dale Donald; Sampson, Sheri L.; Vincenzo, Terry 2004. Corrosion Protection of Ductile Iron Pipe. *Corrosion (2004) - Conference*. 1–17. doi:10.1061/40745(146)75.

Muntakim, A.H., and Dhar, A.S. 2018. Investigation of axial pullout behaviour of buried polyethylene pipelines. Newsletter, International Association for computer methods and advances in Geomechanics, Vol. 23.

Murugathasan, P., Dhar, A. and Hawlader, B. 2018. A laboratory facility for studying pullout behaviour of buried pipelines. Annual conference of Canadian Geotechnical Society, GeoEdmonton2018, AB, Canada.

Paulin, M. J., Phillips, R., Clark, J. I., Trigg, A., and Konuk, I.1998. A full-scale investigation into pipeline/soil interaction, International pipeline conference ’98, ASME, Calgary, Alberta, Canada, 2: 779–788.

Phillips, R., Nobahar, A. and Zhou, J. 2004. Combined Axial and Lateral Pipe-Soil Interaction Relationships, International Pipeline Conference IPC2004, ASME, Calgary, Alberta, Canada, 1, 2, and 3: 299–303.

Pike, K. and Kenny, S. 2012. Lateral-Axial Pipe/Soil Interaction Events: Numerical Modelling Trends and Technical Issues, International Pipeline Conference IPC2012, ASME, Calgary, Alberta, Canada, 4: 1–6.

Randolph, M.F., Dolwin, R., and Beck, R. 1994. Design of driven piles in sand. Géotechnique, **44**(3): 427–448. doi.org/10.1680/geot.1994.44.3.427.

Roy, K., Hawlader, B., Kenny, S. and Moore, I., 2015. Finite element modeling of lateral pipeline–soil interactions in dense sand. Canadian Geotechnical Journal, **53**(3): 490–504. doi.org/10.1139/cgj-2015-0171.

Robert, D., Soga, K. and O'Rourke, T. 2016a. Pipelines subjected to fault movement in dry and unsaturated soils, International Journal of Geomechanics, **16**(5): C4016001-1–16.

Robert, D., Soga, K., O'Rourke, T. and Sakanoue, T. 2016b. Lateral load-displacement behaviour of pipelines in unsaturated sands, Journal of Geotechnical and Geoenvironmental Engineering, **142**(11): 04016060-1–13.

Saha, R. C., Dhar, A., Hawlader, B. 2019. Shear strength assessment of a well-graded clean sand. Annual conference of Canadian Geotechnical Society, GeoSt.John's 2019, St.John's, NL, Canada.

Sheil, B. B., Martin, C. M., Byrne, B.W., Plant, M., Williams, K., and Coyne, D. 2018. Full-scale laboratory testing of a buried pipeline in sand subjected to cyclic axial displacements. Géotechnique, **68**(8): 684–698. doi.org/10.1680/jgeot.16.P.275.

Trautmann, C. H. and O'Rouke, T. D. 1985. Lateral force- displacement response of buried pipe, Journal of Geotechnical Engineering, ASCE, **111**(9): 1077-1092.

Trautmann, C. H., O'Rourfce, T. D. and Kulhawy, F. H. 1985. Uplift force- displacement response of buried pipe, Journal of Geotechnical Engineering, **111**(9): 1061–1076.

Tognon, A.R., Rowe, R.K., and Brachman, R.W.I. 1999. Evaluation of sidewall friction for a buried pipe testing facility, Geotextiles and Geomembranes, 17: 193–212.

Uthayakumar, M. 1996. Liquefaction of sands under multiaxial loading. Ph.D. thesis, Department of Civil Engineering, The University of British Columbia, Vancouver, B.C.

Wang, J. and Yang, Z. 2016. Axial friction response of full- scale pipes in soft clays. Applied Ocean Research, 59: 10–23.

Wang, Q., Ye, X., Wang, S., Sloan, S. W., and Sheng, D. 2017. Experimental investigation of compaction-grouted soil nails. Canadian Geotechnical Journal, **54**(12): 1728–1738.

Weerasekara, L., and Wijewickreme, D. 2008. Mobilization of soil loads on buried, polyethylene natural gas pipelines subject to relative axial displacements. Canadian Geotechnical Journal, **45**(9): 1237–1249. doi:10.1139/T08-043.

Wijewickreme, D., Karimian, H., and Honegger, D. 2009. Response of buried steel pipelines subjected to relative axial soil movement. Canadian Geotechnical Journal, **46**(7): 735–752. doi:10.1139/T09-019.

Yimsiri, S., Soga, K., Yoshizaki, K., Dasari, G., and O'Rourke, T. 2004. Lateral and upward soil-pipeline interactions in sand for deep embedment conditions. Journal of Geotechnical and Geo- environmental Engineering, **130**(8):830–842. doi:10.1061/(ASCE)10900241(2004)130:8(830).